

Perturbative Renormalization Factors of Bilinear Operators for Massive Wilson Quarks on the Lattice

Yoshinobu Kuramashi

*Institute of Particle and Nuclear Studies,
High Energy Accelerator Research Organization(KEK),
Tsukuba, Ibaraki 305, Japan*

Abstract

Renormalization factors for local vector and axial vector currents for the Wilson quark action are perturbatively calculated to one loop order including finite quark masses from the ratio of the on-shell quark matrix elements in the Feynman gauge defined on the lattice and in the continuum. For large quark masses of order unity in lattice units, we find that finite quark mass effects are quite large: one-loop coefficients of the renormalization factors differ by 100% compared to those in the massless limit.

1 Introduction

Calculation of weak matrix elements for heavy-light and heavy-heavy mesons represents a subject of great interest in lattice QCD, which is in principle capable of a precise determination of the matrix elements from the first principles. The main source of systematic errors standing in the way to this goal is large $m_q a$ corrections for heavy quark mass m_q in units of the lattice spacing a . In current numerical simulations using the Wilson quark action the magnitude of the b -quark mass in lattice units is of order $m_b a \approx 1 - 2$. To control the large $m_q a$ error lattice studies have to address two problems. One is improvement of the quark action to reduce cut-off effects following either the Symanzik approach[1] or Wilson's renormalization group approach[2]. Another problem is a precise calculation of renormalization factors which relate operators on the lattice to those in the continuum for massive quarks. This calculation may be pursued either by perturbative methods[3] or by non-perturbative one[4]. An improvement of the perturbative calculation including the finite $m_q a$ corrections is the subject of this article.

Renormalization factors connecting the lattice operator to the continuum one consists of the wave-function part and the vertex part. For the wave-function part Kronfeld and Mackenzie argued from the non-relativistic point of view that the tree level normalization of the on-shell wave-function for the Wilson quark action suffers from large $m_q a$ corrections for heavy quark[5]. At the one-loop level, the question of $m_q a$ corrections to the quark self-energy has been addressed by Kronfeld and Mertens for the Wilson quark action in Ref. [6]. For the vertex part there are no $m_q a$ corrections at the tree level on the lattice. At the one-loop level the vertex part has been calculated only in the massless limit so far. For this reason analyses of weak matrix elements so far have to employ the one-loop expression in the massless limit for the renormalization factors combined with the

Kronfeld-Mackenzie normalization at the tree level even for heavy quark masses. For light quark masses $m_q a \ll 1$ we have no doubt that the massless expressions are a good approximation, while for the case of heavy quark masses $m_q a \approx 1$ we may naturally suspect that corrections depending on $m_q a$ is large even at the one-loop level.

The purpose of this paper is to complete the one-loop calculation of the renormalization factors for the vector and axial vector currents for finite quark masses with the Wilson quark action, and to use the results to investigate the magnitude of $m_q a$ corrections at the one-loop level. We calculate the renormalization factors of the bilinear operators from the ratio of the on-shell quark matrix elements in the Feynman gauge defined in the lattice regularization scheme and in the continuum for various combinations of the two external quark masses. For the continuum regularization scheme we employ the naive dimensional regularization(NDR) with the $\overline{\text{MS}}$ subtraction. In order to regularize infrared(IR) divergences which are generated in one-loop contributions for the on-shell wave-function renormalization factor and the vertex corrections, we supply a fictitious mass λ to the gluon propagator both for the lattice scheme and the continuum one. For the lattice scheme we extract the one-loop terms independent of λ following the method used for the massless case in Ref. [7].

This paper is organized as follows. In Sec. 2 we give the lattice and continuum Feynman rules, and describe the strategy for one-loop calculation of renormalization factors of the bilinear operators for finite quark masses. In Sec. 3 we demonstrate the technique to extract the one-loop terms independent of λ for the lattice on-shell wave-function renormalization factor, and present one-loop results for the relation between the lattice and continuum on-shell wave-function renormalization factors. Results for one-loop relations between the lattice vertex functions and the continuum ones are given in Sec. 4. In Sec. 5 we present results for the renormalization factors of the vector and axial vector currents and discuss the magnitude of

$m_q a$ corrections at the one-loop level. Our conclusions are summarized in Sec. 6.

Throughout this paper we use the same notation for quantities defined on the lattice and their counterparts in the continuum. However, in case of any possibility of confusion, we shall make a clear distinction between them.

2 Formalism

2.1 Feynman rules

The partition function of the lattice theory defined on a four-dimensional Euclidean space-time lattice with lattice spacing a is given by

$$Z = \int \Pi_{x,\mu} \mathcal{D}U_\mu(x) \Pi_{x,f} \mathcal{D}\bar{\psi}_f(x) \mathcal{D}\psi_f(x) \exp[-S_G - S_W], \quad (1)$$

where sites are labeled by $x \equiv (n_1 a, n_2 a, n_3 a, n_4 a)$ with n_1, \dots, n_4 integers. We take the standard Wilson gauge action for SU(3) gauge link variables $U_\mu(x)$ given by

$$S_G = -\frac{1}{g^2} \sum_{x,\mu,\nu} \text{ReTr} [U_\mu(x) U_\nu(x + \hat{\mu}) U_\mu^\dagger(x + \hat{\nu}) U_\nu^\dagger(x)] \quad (2)$$

with the bare coupling constant g . For the quark fields $\bar{\psi}_f(x)$ and $\psi_f(x)$ the Wilson quark action is given by

$$S_W = a^4 \sum_{x,f} \left\{ \left(m_f + \frac{4r}{a} \right) \bar{\psi}_f(x) \psi_f(x) - \frac{1}{2a} \sum_\mu \left[\bar{\psi}_f(x + \hat{\mu}) (r + \gamma_\mu) U_\mu^\dagger(x) \psi_f(x) + \bar{\psi}_f(x) (r - \gamma_\mu) U_\mu(x) \psi_f(x + \hat{\mu}) \right] \right\}, \quad (3)$$

where $\hat{\mu}$ is a vector with length a pointing along the μ -direction, m_f is the bare quark mass for each flavor f and r is the Wilson parameter. Color and spin indices are suppressed. We define the Euclidean gamma matrices in terms of the usual Minkowski matrices in the Bjorken-Drell convention according to $\gamma_0 = \gamma_{BD}^0$, $\gamma_j = -i\gamma_{BD}^j$, $\gamma_5 = \gamma_{BD}^5$; they obey $\{\gamma_\mu, \gamma_\nu\} = 2\delta_{\mu\nu}$ and $\gamma_\mu^\dagger = \gamma_\mu$.

Gauge link variables are elements of SU(3) group in the fundamental representation. They can be written in the form

$$U_\mu(x) = \exp \left[iag \sum_A T_A G_\mu^A(x) \right], \quad (4)$$

where T_A ($A = 1, \dots, 8$) are the generators of $SU(3)$ group in the fundamental representation, which are normalized by $\text{Tr}(T_A T_B) = \delta_{AB}/2$, and $G_\mu^A(x)$ are the gluon fields. In order to derive the Feynman rules we expand the link variable $U_\mu(x)$ in terms of the coupling constant g . Higher order terms of $iag \sum_A T_A G_\mu^A(x)$ in the expansion of $U_\mu(x)$ yield tadpole graphs, if powers of $G_\mu^A(x)$ are contracted with each other. These tadpole contributions are suppressed only by powers of g^2 because of cancellations between powers of a from the expansion and ultraviolet divergences. As a result, coefficients in the perturbative expansion in g^2 are large, and lattice perturbation theory does not converge well. To avoid this problem we isolate the tadpole contributions as an overall constant u_0 for the expansion of the link variable $U_\mu(x)$ in terms of g :

$$U_\mu(x) = u_0 \left[1 + iag \sum_A T_A G_\mu^A(x) \right] + O(a^2), \quad (5)$$

where u_0 is the expectation value of the link operator in the gauge employed for perturbative calculations[8].

From now on throughout this paper we use lattice units for expressing physical quantities and suppress the lattice spacing a unless necessary.

We summarize the lattice Feynman rules as follows. The gluon propagator in the Feynman gauge with momentum k is given by

$$\delta_{AB} \delta_{\mu\nu} u_0^4 D(k, \lambda), \quad (6)$$

where

$$D(k, \lambda)^{-1} = 4 \sum_\alpha \sin^2(k_\alpha/2) + \lambda^2. \quad (7)$$

Here, we give the gluon a small mass λ , where eventually $\lambda \rightarrow 0$, to regularize possible IR divergences in one-loop diagrams. The quark propagator with momentum k takes the form

$$S^{-1}(k, m_u, r) = u_0 \left[i \sum_\alpha \gamma_\alpha \sin(k_\alpha) + m_u + 2r \sum_\alpha \sin^2(k_\alpha/2) \right] \quad (8)$$

with $m_u = (m + 4r - 4ru_0)/u_0$. The one-gluon vertex with incoming quark momentum p and outgoing momentum q has the following expression,

$$-gT_A u_0 v_\mu(p/2 + q/2, r), \quad (9)$$

where

$$v_\mu(k, r) = i\gamma_\mu \cos(k_\mu) + r \sin(k_\mu) \quad (10)$$

with no sum over μ . At the one-loop level the two-gluon vertex appears only through gluon tadpole diagrams whose contributions are included in u_0 .

The corresponding continuum Feynman rules are as follows: the gluon propagator in the Feynman gauge is $\delta_{AB}\delta_{\mu\nu}\tilde{D}(k, \lambda)$ with $\tilde{D}(k, \lambda)^{-1} = k^2 + \lambda^2$, the quark propagator is given by $\tilde{S}^{-1}(k, m) = (i\not{k} + m)$, where \not{k} denotes $\sum_\alpha \gamma_\alpha k_\alpha$, and the quark-gluon vertex is $-gT_A \tilde{v}_\mu$ with $\tilde{v}_\mu = i\gamma_\mu$.

2.2 Procedure of calculation

In the lattice regularization scheme ultraviolet divergences of composite operators are regularized by the cutoff a^{-1} , while in the NDR scheme in the continuum this is achieved by a reduction of the space-time dimension from four. Operators defined in each regularization scheme can be related by renormalization factors which are expected to converge for the perturbative expansion in terms of $\alpha_s = g^2/(4\pi)$ due to the asymptotic freedom of the theory. For the vector and axial vector currents the relation takes the form,

$$\left(\bar{\psi}_2(x)\gamma_\mu\psi_1(x)\right)^{\text{cont}} = Z_{V_\mu} \left(\bar{\psi}_2(x)\gamma_\mu\psi_1(x)\right)^{\text{latt}}, \quad (11)$$

$$\left(\bar{\psi}_2(x)\gamma_\mu\gamma_5\psi_1(x)\right)^{\text{cont}} = Z_{A_\mu} \left(\bar{\psi}_2(x)\gamma_\mu\gamma_5\psi_1(x)\right)^{\text{latt}}, \quad (12)$$

with Z_{V_μ} and Z_{A_μ} ($\mu = 1, \dots, 4$) renormalization factors.

A possible way to perturbatively determine Z_{V_μ} and Z_{A_μ} is to calculate the ratio of the matrix elements for the lattice and continuum regularization schemes employing external on-shell quark or anti-quark states in the Feynman gauge.

For the vector and axial vector matrix elements we further need to specify space momenta of external quark or anti-quark states since the matrix elements generally depend on them. We take the natural choice of zero spatial momentum in this article. The renormalization constants are then calculated from

$$Z_{V_i} = \frac{\langle \bar{q}_2 | \bar{\psi}_2(x) \gamma_i \psi_1(x) | q_1 \rangle^{\text{cont}}}{\langle \bar{q}_2 | \bar{\psi}_2(x) \gamma_i \psi_1(x) | q_1 \rangle^{\text{latt}}} \quad (i = 1, 2, 3), \quad (13)$$

$$Z_{V_4} = \frac{\langle q_2 | \bar{\psi}_2(x) \gamma_4 \psi_1(x) | q_1 \rangle^{\text{cont}}}{\langle q_2 | \bar{\psi}_2(x) \gamma_4 \psi_1(x) | q_1 \rangle^{\text{latt}}}, \quad (14)$$

$$Z_{A_i} = \frac{\langle q_2 | \bar{\psi}_2(x) \gamma_i \gamma_5 \psi_1(x) | q_1 \rangle^{\text{cont}}}{\langle q_2 | \bar{\psi}_2(x) \gamma_i \gamma_5 \psi_1(x) | q_1 \rangle^{\text{latt}}} \quad (i = 1, 2, 3), \quad (15)$$

$$Z_{A_4} = \frac{\langle \bar{q}_2 | \bar{\psi}_2(x) \gamma_4 \gamma_5 \psi_1(x) | q_1 \rangle^{\text{cont}}}{\langle \bar{q}_2 | \bar{\psi}_2(x) \gamma_4 \gamma_5 \psi_1(x) | q_1 \rangle^{\text{latt}}}, \quad (16)$$

where q and \bar{q} stand for quark and anti-quark respectively. The choice of a quark state $\langle q_2 |$ or an anti-quark state $\langle \bar{q}_2 |$ for the external state is made to ensure a non-zero value of the matrix element for each operator. We should note that because of violation of space-time permutation symmetry in our choice of momenta for external quark or anti-quark states $Z_{V_i} \neq Z_{V_4}$ and $Z_{A_i} \neq Z_{A_4}$ are expected due to possible $m_q a$ corrections except in the limit of $a \rightarrow 0$.

At the tree level on-shell wave-function renormalization factor for the Wilson quark action is shifted from unity by finite $m_q a$ corrections[5]

$$\begin{aligned} Z_{V_i}^{(0)} &= Z_{V_4}^{(0)} = Z_{A_i}^{(0)} = Z_{A_4}^{(0)} \\ &= u_0 \sqrt{\cosh(E_1^{(0)}) + r \sinh(E_1^{(0)})} \sqrt{\cosh(E_2^{(0)}) + r \sinh(E_2^{(0)})}, \end{aligned} \quad (17)$$

where $E^{(0)}$ denotes the pole mass at the tree level in common between the Wilson quark action and the continuum one. The superscript (i) refers to the i -th loop level. Up to the one-loop level renormalization factors are written as

$$Z_{V_i} = Z_{V_i}^{(0)} [1 + \alpha_s \Delta_{V_i}], \quad (18)$$

$$Z_{V_4} = Z_{V_4}^{(0)} [1 + \alpha_s \Delta_{V_4}], \quad (19)$$

$$Z_{A_i} = Z_{A_i}^{(0)} [1 + \alpha_s \Delta_{A_i}], \quad (20)$$

$$Z_{A_4} = Z_{A_4}^{(0)} [1 + \alpha_s \Delta_{A_4}], \quad (21)$$

with

$$\Delta_{V_\mu} = \frac{\Delta_{\psi_1}}{2} + \frac{\Delta_{\psi_2}}{2} + \Delta_{\gamma_\mu}, \quad (22)$$

$$\Delta_{A_\mu} = \frac{\Delta_{\psi_1}}{2} + \frac{\Delta_{\psi_2}}{2} + \Delta_{\gamma_\mu \gamma_5}, \quad (23)$$

where Δ_ψ is the difference at the one-loop level between the lattice and continuum on-shell wave-function renormalization factors, and Δ_Γ ($\Gamma = \gamma_\mu, \gamma_\mu \gamma_5$) are a similar difference for the vertex functions. We remark that Δ_ψ and Δ_Γ are functions of $E_1^{(0)}$, $E_2^{(0)}$ and r . In the following two sections we present our calculation of Δ_ψ and Δ_Γ , and examine their pole mass dependences.

3 Quark self-energy

3.1 Lattice results

The one-loop diagram for the quark self-energy is shown in Fig. 1, where external quarks have zero spatial momentum. Using the lattice Feynman rules in Sec. 2 we can write the one-loop contribution as

$$\frac{\alpha_s}{u_0^3} \Sigma^{(1)}(p_4, m_u, r) = \frac{\alpha_s}{u_0^3} \int_{-\pi}^{\pi} \frac{d^4 k}{(2\pi)^4} I_\psi(k, p_4, m_u, r) \quad (24)$$

with

$$I_\psi(k, p_4, m_u, r) = 4\pi C_F \sum_\rho v_\rho(p_4 + k/2, r) S(p_4 + k, m_u, r) v_\rho(p_4 + k/2, r) D(k, \lambda), \quad (25)$$

where $C_F = 4/3$ is the quadratic Casimir invariant for the fundamental representation of SU(3) group. The one-loop self-energy $\Sigma^{(1)}$ consists of the kinetic and mass parts;

$$\Sigma^{(1)}(p_4, m_u, r) = i\gamma_4 \sin(p_4) \Sigma_p^{(1)}(p_4, m_u, r) + \Sigma_m^{(1)}(p_4, m_u, r). \quad (26)$$

With this expression the inverse of the quark propagator up to the one-loop level is given by

$$S^{-1}(p_4, m_u, r) = u_0 \left\{ i\gamma_4 \sin(p_4) \left[1 - \frac{\alpha_s}{u_0^4} \Sigma_p^{(1)}(p_4, m_u, r) \right] + m_u + 2r \sin^2(p_4/2) - \frac{\alpha_s}{u_0^4} \Sigma_m^{(1)}(p_4, m_u, r) \right\}. \quad (27)$$

Since the quark mass is additively renormalized at the one-loop level due to the chiral symmetry breaking term in the Wilson quark action, on-shell condition for massless quark takes the form $S^{-1}(p_4 = 0, m_u^c, r) = 0$. Here the critical quark mass m_u^c measures the magnitude of the additive renormalization. It is determined by the integral equation

$$m_u^c = \frac{\alpha_s}{u_0^4} \Sigma_m^{(1)}(p_4 = 0, m_u^c, r) \quad (28)$$

$$= \frac{\alpha_s}{u_0^4} \int_{-\pi}^{\pi} \frac{d^4 k}{(2\pi)^4} 4\pi C_F \frac{[m_u^c + 2r\Delta_1] \Delta_6(r) + r\Delta_4}{4\Delta_1 \left\{ \Delta_4 + [m_u^c + 2r\Delta_1]^2 \right\}}, \quad (29)$$

where, following the notation of Ref.[7],

$$\Delta_1 = \sum_{\alpha} \sin^2(k_{\alpha}/2), \quad (30)$$

$$\Delta_4 = \sum_{\alpha} \sin^2(k_{\alpha}), \quad (31)$$

$$\Delta_6(r) = (1 + r^2)\Delta_1 - 4. \quad (32)$$

Using m_u^c we can transform (27) into the following form

$$\begin{aligned} S^{-1}(p_4, m_u, r) = u_0 \left\{ i\gamma_4 \sin(p_4) \left[1 - \frac{\alpha_s}{u_0^4} \Sigma_p^{(1)}(p_4, m_u, r) \right] + m_u - m_u^c \right. \\ \left. + 2r \sin^2(p_4/2) - \frac{\alpha_s}{u_0^4} \Sigma_m^{(1)}(p_4, m_u, r) + \frac{\alpha_s}{u_0^4} \Sigma_m^{(1)}(p_4 = 0, m_u^c, r) \right\}. \end{aligned} \quad (33)$$

Up to the one-loop level this expression is equivalent to

$$\begin{aligned} S^{-1}(p_4, \hat{m}_u, r) = u_0 \left\{ i\gamma_4 \sin(p_4) \left[1 - \frac{\alpha_s}{u_0^4} \Sigma_p^{(1)}(p_4, \hat{m}_u, r) \right] + \hat{m}_u \right. \\ \left. + 2r \sin^2(p_4/2) - \frac{\alpha_s}{u_0^4} \hat{\Sigma}_m^{(1)}(p_4, \hat{m}_u, r) \right\}, \end{aligned} \quad (34)$$

where

$$\hat{m}_u = m_u - m_u^c, \quad (35)$$

$$\hat{\Sigma}_m^{(1)}(p_4, \hat{m}_u, r) = \Sigma_m^{(1)}(p_4, \hat{m}_u, r) - \Sigma_m^{(1)}(0, 0, r), \quad (36)$$

with $m_u^c = \Sigma_m^{(1)}(0, 0, r)$. We should note that, defining \hat{m}_u as the bare quark mass, (34) satisfies the on-shell condition for massless quark up to the one-loop level. We

consider that \hat{m}_u corresponds to the quark mass non-perturbatively determined from vanishing pion mass in Monte Carlo simulations. In the following analysis we use \hat{m}_u as the bare quark mass.

The pole mass E is given by the pole of the quark propagator; $S^{-1}(p_4 = iE, \hat{m}_u, r) = 0$. At the tree-level the equation

$$S^{-1}(p_4 = iE^{(0)}, \hat{m}_u, r) = u_0 \left\{ -\gamma_4 \sinh(E^{(0)}) + \hat{m}_u - 2r \sinh^2(E^{(0)}/2) \right\} = 0 \quad (37)$$

determines

$$E^{(0)} = \ln \left| \frac{\hat{m}_u + r + \sqrt{\hat{m}_u^2 + 2r\hat{m}_u + 1}}{1 + r} \right|. \quad (38)$$

One-loop correction is obtained by finding the pole of the quark propagator (34).

Defining the one-loop term by

$$E = E^{(0)} + \frac{\alpha_s}{u_0^4} E^{(1)}(E^{(0)}, r), \quad (39)$$

we find

$$\begin{aligned} & \frac{\alpha_s}{u_0^4} E^{(1)}(E^{(0)}, r) \\ = & \frac{\alpha_s \sinh(E^{(0)}) \Sigma_p^{(1)}(p_4 = iE^{(0)}, \hat{m}_u, r) - \hat{\Sigma}_m^{(1)}(p_4 = iE^{(0)}, \hat{m}_u, r)}{u_0^4 \cosh(E^{(0)}) + r \sinh(E^{(0)})}. \end{aligned} \quad (40)$$

In Table. 1 we present numerical values of $E^{(1)}$ evaluated with $r = 1$ using the Monte Carlo integration routine BASES[9] for representative values of $E^{(0)}$. The numerical accuracy is better than 2%. Fig. 2 illustrate the $E^{(0)}$ dependence of $E^{(1)}$.

The on-shell wave-function renormalization factor is defined as the residue of the quark propagator;

$$Z_\psi^{-1}(E, r) = \left. \frac{\partial S^{-1}(p_4, \hat{m}_u, r)}{i \partial(p_4 \gamma_4)} \right|_{p_4 \gamma_4 = iE}. \quad (41)$$

In terms of the expression (34) Z_ψ^{-1} is written up to the one-loop level as

$$Z_\psi^{-1}(E^{(0)}, r) = u_0 [\cosh(E) + r \sinh(E)] - \frac{\alpha_s}{u_0^3} \left. \frac{\partial \Sigma^{(1)}(p_4, \hat{m}_u, r)}{i \partial(p_4 \gamma_4)} \right|_{p_4 \gamma_4 = iE^{(0)}}, \quad (42)$$

where E is given by (39) and

$$\Sigma^{(1)}(p_4, \hat{m}_u, r) = i\gamma_4 \sin(p_4) \Sigma_p^{(1)}(p_4, \hat{m}_u, r) + \hat{\Sigma}_m^{(1)}(p_4, \hat{m}_u, r). \quad (43)$$

Even at the tree-level the on-shell wave-function renormalization factor suffers from finite $m_q a$ corrections as is clear from

$$Z_\psi^{(0)-1}(E^{(0)}, r) = u_0 [\cosh(E^{(0)}) + r \sinh(E^{(0)})]. \quad (44)$$

Factorizing the tree level contribution we obtain the following expression

$$\begin{aligned} \frac{Z_\psi^{-1}(E^{(0)}, r)}{Z_\psi^{(0)-1}(E^{(0)}, r)} &= 1 + \frac{\alpha_s}{u_0^4} \frac{\sinh(E^{(0)}) + r \cosh(E^{(0)})}{\cosh(E^{(0)}) + r \sinh(E^{(0)})} E^{(1)}(E^{(0)}, r) \\ &\quad - \frac{\alpha_s}{u_0^4} \frac{1}{\cosh(E^{(0)}) + r \sinh(E^{(0)})} \frac{\partial \Sigma^{(1)}(p_4, \hat{m}_u, r)}{i \partial(p_4 \gamma_4)} \Big|_{p_4 \gamma_4 = i E^{(0)}}. \end{aligned} \quad (45)$$

Applying the power counting rule we note that the right-hand side has an IR divergence for $\lambda \rightarrow 0$ arising from the third term. To extract the terms independent of λ we consider subtracting from the integrand of the third term an analytically integrable expression which has the same IR behavior in the region of small loop momentum k ;

$$\begin{aligned} &\frac{1}{\cosh(E^{(0)}) + r \sinh(E^{(0)})} \frac{\partial \Sigma^{(1)}(p_4, \hat{m}_u, r)}{i \partial(p_4 \gamma_4)} \Big|_{p_4 \gamma_4 = i E^{(0)}} \\ &= \int_{-\pi}^{\pi} \frac{d^4 k}{(2\pi)^4} \frac{\partial \tilde{I}_\psi(k, p_4, E^{(0)})}{i \partial(p_4 \gamma_4)} \Big|_{p_4 \gamma_4 = i E^{(0)}} \\ &\quad + \int_{-\pi}^{\pi} \frac{d^4 k}{(2\pi)^4} \frac{\partial}{i \partial(p_4 \gamma_4)} \left[\frac{I_\psi(k, p_4, \hat{m}_u, r)}{\cosh(E^{(0)}) + r \sinh(E^{(0)})} - \tilde{I}_\psi(k, p_4, E^{(0)}) \right] \Big|_{p_4 \gamma_4 = i E^{(0)}, \lambda=0}, \end{aligned} \quad (46)$$

where the IR behavior of

$$\frac{\partial}{i \partial(p_4 \gamma_4)} \tilde{I}_\psi(k, p_4, E^{(0)}) \Big|_{p_4 \gamma_4 = i E^{(0)}, \lambda=0} \quad (47)$$

is the same as that of

$$\frac{\partial}{i \partial(p_4 \gamma_4)} \frac{I_\psi(k, p_4, \hat{m}_u, r)}{\cosh(E^{(0)}) + r \sinh(E^{(0)})} \Big|_{p_4 \gamma_4 = i E^{(0)}, \lambda=0}. \quad (48)$$

In this expression the IR divergence is transferred to the first term, and in consequence the second term is finite. For the candidate of \tilde{I}_ψ we try the continuum

counterpart of the integrand $I_\psi/[\cosh(E^{(0)}) + r\sinh(E^{(0)})]$ replacing $v_\rho(p_4 + k/2, r)$ by \tilde{v}_ρ , $S(p_4 + k, m_u, r)$ by $\tilde{S}(p_4 + k, E^{(0)})$ and $D(k, \lambda)$ by $\tilde{D}(k, \lambda)$ in (25),

$$\tilde{I}_\psi(k, p_4, E^{(0)}) = \theta(\Lambda^2 - k^2) 4\pi C_F \sum_\rho \tilde{v}_\rho \tilde{S}(p_4 + k, E^{(0)}) \tilde{v}_\rho \tilde{D}(k, \lambda), \quad (49)$$

where the domain of integration is restricted to a hyper-sphere of radius Λ , not exceeding π , for convenience of an analytical integration. It is apparent that in the limit of $a \rightarrow 0$ (47) and (48) have the same IR behavior. At a finite lattice spacing, however, the IR behaviors of the two integrands are different due to finite $m_q a$ corrections.

Let us examine the IR behaviors of the denominators of (47) and (48), where we transfer the Dirac structure in the denominators of quark propagators to the numerators. For the continuum case we find

$$\begin{aligned} & \tilde{D}^{-1}(k, \lambda = 0) \left[\tilde{S}^{-1}(p_4 + k, E^{(0)}) \tilde{S}^{-1}(-(p_4 + k), E^{(0)}) \right]^2 \\ &= k^2 \left[i2k_4 E^{(0)} + k^2 \right]^2 \end{aligned} \quad (50)$$

with the use of the on-shell condition $p_4^2 = -E^{(0)2}$. For the lattice case we expand the quark and gluon propagators around $k = 0$, obtaining

$$\begin{aligned} & \left[\cosh(E^{(0)}) + r\sinh(E^{(0)}) \right] D^{-1}(k, \lambda = 0) \\ & \times \left\{ S^{-1}(p_4 + k, \hat{m}_u, r) S^{-1}(-(p_4 + k), \hat{m}_u, r) \right\}^2 \\ &= \left[\cosh(E^{(0)}) + r\sinh(E^{(0)}) \right] \left[k^2 + O(k^4) \right] \\ & \times \left\{ i2k_4 \sinh(E^{(0)}) \left[\cosh(E^{(0)}) + r\sinh(E^{(0)}) \right] + k^2(1 + r\sinh(E^{(0)})) \right. \\ & \left. + k_4^2 \sinh(E^{(0)}) \left[(2 - r^2)\sinh(E^{(0)}) + r(\cosh(E^{(0)}) - 1) \right] + O(k^3) \right\}^2, \end{aligned} \quad (51)$$

where the on-shell condition of external quark is used. While the two expressions above show a different IR behavior, the difference can be absorbed, aside from an overall factor, by replacing the pole mass $E^{(0)}$ in (50) by

$$\tilde{m} = \sinh(E^{(0)}) \frac{\cosh(E^{(0)}) + r\sinh(E^{(0)})}{1 + r\sinh(E^{(0)})}. \quad (52)$$

Here, we do not take account of the last term in (51) because it does not give leading order contributions either for the case of $k_4 = 0$ or of $k_4 \neq 0$ for small k . It is straightforward to check that the remaining overall $m_q a$ corrections of the denominator are precisely canceled with those arising from the numerator with $k = 0$.

Consequently we take for the integrand \tilde{I}_ψ the following expression,

$$\tilde{I}_\psi(k, p_4, \tilde{m}) = \theta(\Lambda^2 - k^2) 4\pi C_F \sum_{\rho} \tilde{v}_\rho \tilde{S}(p_4 + k, \tilde{m}) \tilde{v}_\rho \tilde{D}(k, \lambda). \quad (53)$$

A simple calculation gives

$$\begin{aligned} & \int_{-\pi}^{\pi} \frac{d^4 k}{(2\pi)^4} \frac{\partial \tilde{I}_\psi(k, p_4, \tilde{m})}{i\partial(p_4 \gamma_4)} \Big|_{p_4 \gamma_4 = i\tilde{m}} \\ &= \frac{C_F}{4\pi} \left\{ -2 \ln \left| \frac{\lambda^2}{\Lambda^2} \right| - \frac{3\Lambda^4}{4\tilde{m}^4} - \frac{9\Lambda}{2\tilde{m}^2} \sqrt{\Lambda^2 + 4\tilde{m}^2} + \frac{3\Lambda}{4\tilde{m}^4} (\Lambda^2 + 4\tilde{m}^2)^{\frac{3}{2}} \right. \\ & \quad \left. - 6 \ln \left| \frac{\Lambda + \sqrt{\Lambda^2 + 4\tilde{m}^2}}{2\tilde{m}} \right| \right\}, \end{aligned} \quad (54)$$

whose massless limit is

$$\lim_{\tilde{m} \rightarrow 0} \int_{-\pi}^{\pi} \frac{d^4 k}{(2\pi)^4} \frac{\partial \tilde{I}_\psi(k, p_4, \tilde{m})}{i\partial(p_4 \gamma_4)} \Big|_{p_4 \gamma_4 = i\tilde{m}} = \frac{C_F}{4\pi} \left\{ -\ln \left| \frac{\Lambda^2}{\tilde{m}^2} \right| - 2 \ln \left| \frac{\lambda^2}{\tilde{m}^2} \right| - \frac{9}{2} \right\}, \quad (55)$$

where λ is assumed to be less than \tilde{m} .

3.2 Continuum results

We turn to the calculation of the on-shell wave-function renormalization factor using the continuum NDR scheme instead of the lattice regularization scheme. For the one-loop contribution to the quark self-energy shown in Fig. 1 the continuum Feynman rules in Sec. 2 give the expression

$$\alpha_s \Sigma^{(1)}(p, m) = \alpha_s \int_{-\infty}^{\infty} \frac{d^D k}{(2\pi)^D} 4\pi C_F \sum_{\rho} \tilde{v}_\rho \tilde{S}(p + k, m) \tilde{v}_\rho \tilde{D}(k, \lambda), \quad (56)$$

where D is the reduced space-time dimension which is parameterized by ϵ as

$$D = 4 - \epsilon, \quad \epsilon > 0. \quad (57)$$

Since this dimensional reduction procedure prevents us from taking zero spatial momentum for the external quark state before the loop integration, we perform the calculation of the on-shell wave-function renormalization factor in a Euclidean invariant way.

Up to one-loop corrections the quark propagator takes the form

$$\tilde{S}^{-1}(p, m) = i\not{p} + m - \alpha_s \Sigma^{(1)}(p, m). \quad (58)$$

In terms of this expression the on-shell wave-function renormalization factor Z_ψ^{-1} is written up to the one-loop level as

$$Z_\psi^{-1}(m) = 1 - \alpha_s \left. \frac{\partial \Sigma^{(1)}(p, m)}{i \partial \not{p}} \right|_{\not{p}=im}. \quad (59)$$

At the tree level we find

$$Z_\psi^{(0)-1}(m) = 1. \quad (60)$$

Performing the integration in an elementary way we obtain the one-loop correction

$$\begin{aligned} & \left. \frac{\partial \Sigma^{(1)}(p, m)}{i \partial \not{p}} \right|_{\not{p}=im} \\ &= \frac{C_F}{4\pi} \left[- \left(\frac{2}{\epsilon} - \gamma + \ln |4\pi| \right) - \ln \left| \frac{\mu^2}{m^2} \right| - 2 \ln \left| \frac{\lambda^2}{m^2} \right| - 4 \right], \end{aligned} \quad (61)$$

where the pole term $(2/\epsilon - \gamma + \ln |4\pi|)$ should be eliminated in the $\overline{\text{MS}}$ scheme. We note that this result is independent of the choice of spatial momenta for the external quark state because of Euclidean invariance in the continuum theory.

3.3 Relation between continuum and lattice wave-function renormalization factors

Using the results for the lattice and continuum wave-function renormalization factors obtained in the previous subsections, let us find the correction factor which connects the two factors. From (44) and (60) the tree-level relation is

$$Z_\psi^{(0)\text{cont}}(m) = u_0 \left[\cosh(E^{(0)}) + r \sinh(E^{(0)}) \right] Z_\psi^{(0)\text{latt}}(E^{(0)}, r), \quad (62)$$

where we take $m = E^{(0)}$. Up to the one-loop level we obtain the following expression

$$Z_\psi^{\text{cont}}(m) = u_0 \left[\cosh(E^{(0)}) + r \sinh(E^{(0)}) \right] \left[1 + \alpha_s \Delta_\psi(E^{(0)}, r) \right] Z_\psi^{\text{latt}}(E^{(0)}, r), \quad (63)$$

where, from (45) and (59),

$$\Delta_\psi(E^{(0)}, r) = \frac{\partial \Sigma^{(1)\text{cont}}(p, m)}{i \partial \not{p}} \Big|_{\not{p}=im} + \frac{\sinh(E^{(0)}) + r \cosh(E^{(0)})}{\cosh(E^{(0)}) + r \sinh(E^{(0)})} E^{(1)\text{latt}}(E^{(0)}, r) - \frac{1}{\cosh(E^{(0)}) + r \sinh(E^{(0)})} \frac{\partial \Sigma^{(1)\text{latt}}(p_4, \hat{m}_u, r)}{i \partial(p_4 \gamma_4)} \Big|_{p_4 \gamma_4 = i E^{(0)}}, \quad (64)$$

with $m = E^{(0)}$. For the coupling constant we can take either α_s^{cont} or $\alpha_s^{\text{latt}}/u_0^4$ because the difference is of order α_s^2 . From (55) and (61) we observe that the IR singular terms in (64) for $\lambda \rightarrow 0$ are precisely canceled. We also note that the mass singularities occurring at $E^{(0)} \rightarrow 0$ in individual terms of (64) also cancel, which assures us that $\Delta_\psi(E^{(0)}, r)$ is finite even in the massless limit.

In Table 1 we present numerical values of $\Delta_\psi(E^{(0)}, r)$ evaluated using BASES with an inaccuracy of less than 2% for representative values of the pole mass $E^{(0)}$ for the $r = 1$ case. The pole mass dependence of Δ_ψ is shown in Fig. 3. We observe that the $m_q a$ corrections give large contributions in the region $E^{(0)} \gtrsim 0.05$.

4 Vertex functions

4.1 Lattice results

At the tree level the lattice vertex functions for $\Gamma = \gamma_\mu, \gamma_\mu \gamma_5$ ($\mu = 1, \dots, 4$) do not suffer from $m_q a$ corrections, which contrasts with the wave-function case. Up to the one-loop level the vertex functions are written in the following form

$$\Lambda_\Gamma(E_1^{(0)}, E_2^{(0)}, r) = \Gamma + \frac{\alpha_s}{u_0^4} \Lambda_\Gamma^{(1)}(E_1^{(0)}, E_2^{(0)}, r) \quad (65)$$

where $E_1^{(0)}$ and $E_2^{(0)}$ are the pole masses for the external quarks. The one-loop vertex corrections $\Lambda_\Gamma^{(1)}$ for $\Gamma = \gamma_4, \gamma_i \gamma_5$ and $\Gamma = \gamma_i, \gamma_4 \gamma_5$ ($i = 1, 2, 3$) are obtained

by evaluating the diagrams shown in Fig. 4(a) and Fig. 4(b), respectively, on condition that the external quark and anti-quark are on-shell with zero spatial momentum.

We first consider the case of $\Gamma = \gamma_4, \gamma_i \gamma_5$ for which external states are quarks. Using the lattice Feynman rules in Sec. 2, the amplitude corresponding to Fig. 4(a) is expressed as

$$\frac{\alpha_s}{u_0^4} \Lambda_\Gamma^{(1)}(E_1^{(0)}, E_2^{(0)}, r) = \frac{\alpha_s}{u_0^4} \int_{-\pi}^{\pi} \frac{d^4 k}{(2\pi)^4} I_\Gamma(k, E_1^{(0)}, E_2^{(0)}, r), \quad (66)$$

with

$$\begin{aligned} I_\Gamma(k, E_1^{(0)}, E_2^{(0)}, r) &= 4\pi C_F \sum_{\rho} v_{\rho}(p'_4 + k/2, r) S(p'_4 + k, \hat{m}_{2u}, r) \\ &\quad \times \Gamma S(p_4 + k, \hat{m}_{1u}, r) v_{\rho}(p_4 + k/2, r) D(k, \lambda), \end{aligned} \quad (67)$$

where $E_1^{(0)}$ and $E_2^{(0)}$ are expressed with \hat{m}_{1u} and \hat{m}_{2u} , respectively, as in (38). We take the following on-shell conditions for the external quarks

$$\left(i\gamma_4 \sin(p_4) + \hat{m}_{1u} + 2r \sin^2(p_4/2) \right) u(p_4) = 0, \quad (68)$$

$$\bar{u}(p'_4) \left(i\gamma_4 \sin(p'_4) + \hat{m}_{2u} + 2r \sin^2(p'_4/2) \right) = 0, \quad (69)$$

where $u(p_4)$ is the Dirac spinor for the incoming quark state and $\bar{u}(p'_4)$ that for the outgoing quark state. The vertex correction (66) has IR divergences for $\lambda \rightarrow 0$ as can be seen by the power counting. In order to extract the terms independent of λ we subtract from the integrand $I_\Gamma(k, E_1^{(0)}, E_2^{(0)}, r)$ an expression \tilde{I}_Γ which has the same IR behavior near $k = 0$

$$\begin{aligned} \tilde{I}_\Gamma(k, \tilde{m}_1, \tilde{m}_2) &= \theta(\Lambda^2 - k^2) 4\pi C_F \sum_{\rho} \tilde{v}_{\rho} \tilde{S}(p'_4 + k, \tilde{m}_2) \\ &\quad \times \Gamma \tilde{S}(p_4 + k, \tilde{m}_1) \tilde{v}_{\rho} \tilde{D}(k, \lambda), \end{aligned} \quad (70)$$

with

$$\tilde{m}_{1,2} = \sinh(E_{1,2}^{(0)}) \frac{\cosh(E_{1,2}^{(0)}) + r \sinh(E_{1,2}^{(0)})}{1 + r \sinh(E_{1,2}^{(0)})}, \quad (71)$$

as we did for the case of the on-shell wave-function renormalization factor in Sec. 3.

The on-shell conditions for the external quarks are

$$(i\gamma_4 p_4 + \tilde{m}_1) u(p_4) = 0, \quad (72)$$

$$\bar{u}(p'_4) (i\gamma_4 p'_4 + \tilde{m}_2) = 0. \quad (73)$$

Using $\tilde{I}_\Gamma(k, \tilde{m}_1, \tilde{m}_2)$ we can decompose the vertex correction $\Lambda_\Gamma^{(1)}(E_1^{(0)}, E_2^{(0)}, r)$ into an IR divergent part and a finite one;

$$\begin{aligned} \Lambda_\Gamma^{(1)}(E_1^{(0)}, E_2^{(0)}, r) &= \int_{-\pi}^{\pi} \frac{d^4 k}{(2\pi)^4} \tilde{I}_\Gamma(k, \tilde{m}_1, \tilde{m}_2) \\ &+ \int_{-\pi}^{\pi} \frac{d^4 k}{(2\pi)^4} [I_\Gamma(k, E_1^{(0)}, E_2^{(0)}, r) - \tilde{I}_\Gamma(k, \tilde{m}_1, \tilde{m}_2)] \Big|_{\lambda=0}. \end{aligned} \quad (74)$$

We have carried out the first integral analytically and the second one numerically using BASES. The analytical integrations of $\tilde{I}_\Gamma(k, \tilde{m}_1, \tilde{m}_2)$ for $\Gamma = \gamma_4, \gamma_i \gamma_5$ give the following results

$$\begin{aligned} &\int_{-\pi}^{\pi} \frac{d^4 k}{(2\pi)^4} \tilde{I}_{\gamma_4}(k, \tilde{m}_1, \tilde{m}_2) / \left[\frac{C_F}{4\pi} \gamma_4 \right] \\ &= 2 \ln \left| \frac{\lambda^2}{\Lambda^2} \right| + \left\{ - \left(\frac{1}{\tilde{m}_1^2} - \frac{1}{\tilde{m}_1 \tilde{m}_2} \right) \frac{\Lambda^2}{2} + \left(\frac{1}{2\tilde{m}_1^2 \tilde{m}_2^2} + \frac{1}{\tilde{m}_1^3 \tilde{m}_2} \right) \frac{\Lambda^4}{4} \right. \\ &\quad - \frac{\tilde{m}_2}{\tilde{m}_1 - \tilde{m}_2} \left[-4 \frac{\sqrt{\Lambda^2 + 4\tilde{m}_1^2}}{\Lambda} + \frac{\Lambda}{2\tilde{m}_1^2} \sqrt{\Lambda^2 + 4\tilde{m}_1^2} \right. \\ &\quad \left. \left. - \frac{\Lambda}{4\tilde{m}_1^3 \tilde{m}_2} (\Lambda^2 + 4\tilde{m}_1^2)^{\frac{3}{2}} + 6 \ln \left| \frac{\Lambda + \sqrt{\Lambda^2 + 4\tilde{m}_1^2}}{2\tilde{m}_1} \right| \right] + (\tilde{m}_1 \leftrightarrow \tilde{m}_2) \right\} \quad (75) \end{aligned}$$

and

$$\begin{aligned} &\int_{-\pi}^{\pi} \frac{d^4 k}{(2\pi)^4} \tilde{I}_{\gamma_i \gamma_5}(k, \tilde{m}_1, \tilde{m}_2) / \left[\frac{C_F}{4\pi} \gamma_i \gamma_5 \right] \\ &= 2 \ln \left| \frac{\lambda^2}{\Lambda^2} \right| + \left\{ - \left(\frac{1}{\tilde{m}_1^2} + \frac{1}{\tilde{m}_1 \tilde{m}_2} \right) \frac{\Lambda^2}{2} - \left(\frac{1}{2\tilde{m}_1^2 \tilde{m}_2^2} + \frac{1}{\tilde{m}_1^3 \tilde{m}_2} \right) \frac{\Lambda^4}{12} \right. \\ &\quad - \frac{\tilde{m}_2}{\tilde{m}_1 - \tilde{m}_2} \left[-4 \frac{\sqrt{\Lambda^2 + 4\tilde{m}_1^2}}{\Lambda} + \frac{\Lambda}{2\tilde{m}_1^2} \sqrt{\Lambda^2 + 4\tilde{m}_1^2} \right. \\ &\quad \left. \left. + \frac{\Lambda}{12\tilde{m}_1^3 \tilde{m}_2} (\Lambda^2 + 4\tilde{m}_1^2)^{\frac{3}{2}} + 6 \ln \left| \frac{\Lambda + \sqrt{\Lambda^2 + 4\tilde{m}_1^2}}{2\tilde{m}_1} \right| \right] + (\tilde{m}_1 \leftrightarrow \tilde{m}_2) \right\}. \quad (76) \end{aligned}$$

We remark that these expressions do not diverge in the limit of $\tilde{m}_2 \rightarrow \tilde{m}_1$. The results for $\tilde{m}_1 = \tilde{m}_2$ are presented in Appendix.

Let us turn to the second case $\Gamma = \gamma_i, \gamma_4\gamma_5$ for which a quark and an anti-quark have to be chosen for the external states for a non-vanishing matrix element. From Fig. 4(b) we obtain (66) with, however,

$$\begin{aligned} I_\Gamma(k, E_1^{(0)}, E_2^{(0)}, r) &= 4\pi C_F \sum_\rho v_\rho(-p'_4 + k/2, r) S(-p'_4 + k, \hat{m}_{2u}, r) \\ &\quad \times \Gamma S(p_4 + k, \hat{m}_{1u}, r) v_\rho(p_4 + k/2, r) D(k, \lambda). \end{aligned} \quad (77)$$

We assume that the external quark and anti-quark states are on-shell

$$\left(i\gamma_4 \sin(p_4) + \hat{m}_{1u} + 2r \sin^2(p_4/2) \right) u(p_4) = 0, \quad (78)$$

$$\bar{v}(p'_4) \left(-i\gamma_4 \sin(p'_4) + \hat{m}_{2u} + 2r \sin^2(p'_4/2) \right) = 0, \quad (79)$$

where $u(p_4)$ is the Dirac spinor for the incoming quark state and $\bar{v}(p'_4)$ is that for the incoming anti-quark state. We introduce a counter term $\tilde{I}_\Gamma(k, \tilde{m}_1, \tilde{m}_2)$ to regularize the IR singularity of the integrand I_Γ in the vertex correction,

$$\begin{aligned} \tilde{I}_\Gamma(k, \tilde{m}_1, \tilde{m}_2) &= \theta(\Lambda^2 - k^2) 4\pi C_F \sum_\rho \tilde{v}_\rho \tilde{S}(-p'_4 + k, \tilde{m}_2) \\ &\quad \times \Gamma \tilde{S}(p_4 + k, \tilde{m}_1) \tilde{v}_\rho \tilde{D}(k, \lambda) \end{aligned} \quad (80)$$

with $\tilde{m}_{1,2}$ defined in (71). The on-shell conditions for the external quark and anti-quark states used for the counter term are

$$(i\gamma_4 p_4 + \tilde{m}_1) u(p_4) = 0, \quad (81)$$

$$\bar{v}(p'_4) (-i\gamma_4 p'_4 + \tilde{m}_2) = 0. \quad (82)$$

The vertex correction is decomposed to an IR divergent part and a finite one as in (74). The IR divergence resides in the integrations of (80), which are calculated analytically. The finite term is evaluated with numerical integration with the aid of BASES. The results of an analytical integration of (80) for $\Gamma = \gamma_i, \gamma_4\gamma_5$ are as

follows,

$$\begin{aligned}
& \int_{-\pi}^{\pi} \frac{d^4 k}{(2\pi)^4} \tilde{I}_{\gamma_i}(k, \tilde{m}_1, \tilde{m}_2) / \left[\frac{C_F}{4\pi} \gamma_i \right] \\
= & 2 \ln \left| \frac{\lambda^2}{\Lambda^2} \right| + 8 \frac{\pi}{\lambda} \frac{\tilde{m}_1 \tilde{m}_2}{\tilde{m}_1 + \tilde{m}_2} \\
& + \left\{ - \left(\frac{1}{\tilde{m}_1^2} - \frac{1}{\tilde{m}_1 \tilde{m}_2} \right) \frac{\Lambda^2}{2} - \left(\frac{1}{2\tilde{m}_1^2 \tilde{m}_2^2} - \frac{1}{\tilde{m}_1^3 \tilde{m}_2} \right) \frac{\Lambda^4}{12} \right. \\
& + \frac{\tilde{m}_2}{\tilde{m}_1 + \tilde{m}_2} \left[-4 \frac{\sqrt{\Lambda^2 + 4\tilde{m}_1^2}}{\Lambda} + \frac{\Lambda}{2\tilde{m}_1^2} \sqrt{\Lambda^2 + 4\tilde{m}_1^2} \right. \\
& \left. \left. - \frac{\Lambda}{12\tilde{m}_1^3 \tilde{m}_2} (\Lambda^2 + 4\tilde{m}_1^2)^{\frac{3}{2}} + 6 \ln \left| \frac{\Lambda + \sqrt{\Lambda^2 + 4\tilde{m}_1^2}}{2\tilde{m}_1} \right| \right] + (\tilde{m}_1 \leftrightarrow \tilde{m}_2) \right\} \quad (83)
\end{aligned}$$

and

$$\begin{aligned}
& \int_{-\pi}^{\pi} \frac{d^4 k}{(2\pi)^4} \tilde{I}_{\gamma_4 \gamma_5}(k, \tilde{m}_1, \tilde{m}_2) / \left[\frac{C_F}{4\pi} \gamma_4 \gamma_5 \right] \\
= & 2 \ln \left| \frac{\lambda^2}{\Lambda^2} \right| + 8 \frac{\pi}{\lambda} \frac{\tilde{m}_1 \tilde{m}_2}{\tilde{m}_1 + \tilde{m}_2} \\
& + \left\{ - \left(\frac{1}{\tilde{m}_1^2} + \frac{1}{\tilde{m}_1 \tilde{m}_2} \right) \frac{\Lambda^2}{2} + \left(\frac{1}{2\tilde{m}_1^2 \tilde{m}_2^2} - \frac{1}{\tilde{m}_1^3 \tilde{m}_2} \right) \frac{\Lambda^4}{4} \right. \\
& + \frac{\tilde{m}_2}{\tilde{m}_1 + \tilde{m}_2} \left[-4 \frac{\sqrt{\Lambda^2 + 4\tilde{m}_1^2}}{\Lambda} + \frac{\Lambda}{2\tilde{m}_1^2} \sqrt{\Lambda^2 + 4\tilde{m}_1^2} \right. \\
& \left. \left. + \frac{\Lambda}{4\tilde{m}_1^3 \tilde{m}_2} (\Lambda^2 + 4\tilde{m}_1^2)^{\frac{3}{2}} + 6 \ln \left| \frac{\Lambda + \sqrt{\Lambda^2 + 4\tilde{m}_1^2}}{2\tilde{m}_1} \right| \right] + (\tilde{m}_1 \leftrightarrow \tilde{m}_2) \right\}. \quad (84)
\end{aligned}$$

The expressions in the limit of $\tilde{m}_2 \rightarrow \tilde{m}_1$ are listed in Appendix.

4.2 Continuum results

We repeat the calculations of the vertex functions for $\Gamma = \gamma_\mu, \gamma_\mu \gamma_5$ ($\mu = 1, \dots, 4$) in the continuum NDR scheme. The vertex functions up to the one-loop level are written as

$$\Lambda_\Gamma(m_1, m_2) = \Gamma + \alpha_s \Lambda_\Gamma^{(1)}(m_1, m_2). \quad (85)$$

The one-loop contributions $\Lambda_\Gamma^{(1)}$ for $\Gamma = \gamma_4, \gamma_i \gamma_5$ and $\Gamma = \gamma_i, \gamma_4 \gamma_5$ ($i = 1, 2, 3$) are represented in Fig. 4(a) and Fig. 4(b), respectively. We perform the loop

integrations imposing the on-shell conditions on the external quark and anti-quark states in a Euclidean invariant way, and after the integrations set the spatial momenta of the external quark and anti-quark equal to zero.

For the case of $\Gamma = \gamma_4, \gamma_i \gamma_5$ the continuum Feynman rules in Sec. 2 give the following expressions for Fig. 4(a),

$$\begin{aligned} \alpha_s \Lambda_\Gamma^{(1)}(m_1, m_2) &= \alpha_s \int_{-\infty}^{\infty} \frac{d^D k}{(2\pi)^D} 4\pi C_F \sum_{\rho} \tilde{v}_\rho \tilde{S}(p' + k, m_2) \\ &\quad \times \Gamma \tilde{S}(p + k, m_1) \tilde{v}_\rho \tilde{D}(k, \lambda), \end{aligned} \quad (86)$$

where D is the space-time dimension which is reduced from four by ϵ to regularize ultraviolet divergences and Γ is defined as γ_μ or $\gamma_\mu \gamma_5$ for $\mu = 1, 2, \dots, D$. The on-shell conditions for the external quarks are written as

$$(i\not{p} + m_1)u(p) = 0, \quad (87)$$

$$\bar{u}(p')(i\not{p}' + m_2) = 0, \quad (88)$$

where $u(p)$ is the Dirac spinor for incoming quark state and $\bar{u}(p')$ is one for outgoing quark state. After carrying out the integration in (86) we take $\gamma_\mu = \gamma_4$, $\gamma_\mu \gamma_5 = \gamma_i \gamma_5$, $p = (0, 0, 0, im_1)$ and $p' = (0, 0, 0, im_2)$. The final results are given by

$$\begin{aligned} &\Lambda_{\gamma_4}^{(1)}(m_1, m_2) / \left[\frac{C_F}{4\pi} \gamma_4 \right] \\ &= \left(\frac{2}{\epsilon} - \gamma + \ln |4\pi| \right) + \ln \left| \frac{\mu^2}{m_1 m_2} \right| + 2 \ln \left| \frac{\lambda^2}{m_1 m_2} \right| \\ &\quad + 3 \frac{m_1 + m_2}{m_1 - m_2} \ln \left| \frac{m_1}{m_2} \right| - 2 \end{aligned} \quad (89)$$

and

$$\begin{aligned} &\Lambda_{\gamma_i \gamma_5}^{(1)}(m_1, m_2) / \left[\frac{C_F}{4\pi} \gamma_i \gamma_5 \right] \\ &= \left(\frac{2}{\epsilon} - \gamma + \ln |4\pi| \right) + \ln \left| \frac{\mu^2}{m_1 m_2} \right| + 2 \ln \left| \frac{\lambda^2}{m_1 m_2} \right| \\ &\quad + 3 \frac{m_1 + m_2}{m_1 - m_2} \ln \left| \frac{m_1}{m_2} \right| - 4, \end{aligned} \quad (90)$$

where the pole term $(2/\epsilon - \gamma + \ln |4\pi|)$ should be eliminated in the $\overline{\text{MS}}$ scheme. The expressions for $m_2 \rightarrow m_1$ are given in Appendix.

Another case is $\Gamma = \gamma_i, \gamma_4\gamma_5$. The one-loop diagram shown in Fig. 4(b) is written as

$$\begin{aligned} \alpha_s \Lambda_\Gamma^{(1)}(m_1, m_2) &= \alpha_s \int_{-\infty}^{\infty} \frac{d^D k}{(2\pi)^D} 4\pi C_F \sum_{\rho} \tilde{v}_{\rho} \tilde{S}(-p' + k, m_2) \\ &\quad \times \Gamma \tilde{S}(p + k, m_1) \tilde{v}_{\rho} \tilde{D}(k, \lambda), \end{aligned} \quad (91)$$

where the external quark and anti-quark are on-shell

$$(i\not{p} + m_1)u(p) = 0, \quad (92)$$

$$\bar{v}(p')(-i\not{p}' + m_2) = 0, \quad (93)$$

with $\bar{v}(p')$ the Dirac spinor for outgoing anti-quark state. Performing the integration we obtain

$$\begin{aligned} &\Lambda_{\gamma_i}^{(1)}(m_1, m_2) / \left[\frac{C_F}{4\pi} \gamma_i \right] \\ &= \left(\frac{2}{\epsilon} - \gamma + \ln |4\pi| \right) + \ln \left| \frac{\mu^2}{m_1 m_2} \right| + 2 \ln \left| \frac{\lambda^2}{m_1 m_2} \right| + 8 \frac{\pi}{\lambda} \frac{m_1 m_2}{m_1 + m_2} \\ &\quad + 3 \frac{m_1 - m_2}{m_1 + m_2} \ln \left| \frac{m_1}{m_2} \right| - 4 \end{aligned} \quad (94)$$

and

$$\begin{aligned} &\Lambda_{\gamma_4\gamma_5}^{(1)}(m_1, m_2) / \left[\frac{C_F}{4\pi} \gamma_4\gamma_5 \right] \\ &= \left(\frac{2}{\epsilon} - \gamma + \ln |4\pi| \right) + \ln \left| \frac{\mu^2}{m_1 m_2} \right| + 2 \ln \left| \frac{\lambda^2}{m_1 m_2} \right| + 8 \frac{\pi}{\lambda} \frac{m_1 m_2}{m_1 + m_2} \\ &\quad + 3 \frac{m_1 - m_2}{m_1 + m_2} \ln \left| \frac{m_1}{m_2} \right| - 2, \end{aligned} \quad (95)$$

where the pole term $(2/\epsilon - \gamma + \ln |4\pi|)$ should be eliminated in the $\overline{\text{MS}}$ scheme.

4.3 Relation between continuum and lattice vertex functions

From (65) and (85) we obtain the relation between the lattice vertex corrections and the continuum ones up to the one-loop level

$$\Lambda_\Gamma^{\text{cont}}(m_1, m_2) = \left[1 + \alpha_s \Delta_\Gamma(E_1^{(0)}, E_2^{(0)}, r) \right] \Lambda_\Gamma^{\text{latt}}(E_1^{(0)}, E_2^{(0)}, r), \quad (96)$$

with

$$\Delta_\Gamma(E_1^{(0)}, E_2^{(0)}, r) = \Lambda_\Gamma^{(1)\text{cont}}(m_1, m_2) - \Lambda_\Gamma^{(1)\text{latt}}(E_1^{(0)}, E_2^{(0)}, r), \quad (97)$$

where we take $m_1 = E_1^{(0)}$ and $m_2 = E_2^{(0)}$. In Appendix we list the expression for $\Lambda_\Gamma^{(1)\text{cont}}$ and $\Lambda_\Gamma^{(1)\text{latt}}$ in the limit $E_1^{(0)} = E_2^{(0)} \rightarrow 0$ or $E_1^{(0)} \rightarrow 0$. They show that $\Lambda_\Gamma^{(1)\text{latt}}$ and $\Lambda_\Gamma^{(1)\text{cont}}$ have the same singular structures for $\lambda \rightarrow 0$, $E_1^{(0)} = E_2^{(0)} \rightarrow 0$ or $E_1^{(0)} \rightarrow 0$ where we assume $\lambda < E_1^{(0)}, E_2^{(0)}$. Thus Δ_Γ in (97) is IR finite, and also finite in the limit of $E_1^{(0)} = E_2^{(0)} \rightarrow 0$ or $E_1^{(0)} \rightarrow 0$.

Numerical values of $\Delta_\Gamma(E_1^{(0)}, E_2^{(0)}, r)$ for $\Gamma = \gamma_\mu$ evaluated using BASES with an accuracy of better than 2% are tabulated in Table 2 for representative values of the pole masses $E_1^{(0)}$ and $E_2^{(0)}$ for the $r = 1$ case. Fig. 5(a) shows the $E_2^{(0)}$ dependence of Δ_{γ_i} and Δ_{γ_4} for the case of $E_1^{(0)} = E_2^{(0)}$, and Fig. 5(b) is the same as Fig. 5(a) for $E_1^{(0)} = 0$. For both cases we observe that Δ_{γ_i} and Δ_{γ_4} are roughly consistent in the region $E_2^{(0)} \lesssim 0.01$, while as $E_2^{(0)}$ becomes larger the absolute value for Δ_{γ_i} increase and that for Δ_{γ_4} decrease, indicating large $m_q a$ corrections.

Numerical data of $\Delta_\Gamma(E_1^{(0)}, E_2^{(0)}, r)$ for $\Gamma = \gamma_\mu \gamma_5$ are listed in Table 3, which are plotted in Fig. 6(a) for the case of $E_1^{(0)} = E_2^{(0)}$ and in Fig. 6(b) for $E_1^{(0)} = 0$. We observe that $\Delta_{\gamma_i \gamma_5}$ and $\Delta_{\gamma_4 \gamma_5}$ show an $E_2^{(0)}$ dependence similar to that for Δ_{γ_4} and Δ_{γ_i} , respectively.

5 Renormalization factors for vector and axial vector currents

Since we have completed the calculations of Δ_ψ and Δ_Γ ($\Gamma = \gamma_\mu, \gamma_\mu \gamma_5$) we are now ready to discuss the magnitude of finite $m_q a$ corrections in the one-loop contributions of renormalization factors for vector and axial vector currents. Combining the results for Δ_ψ and Δ_Γ we obtain values of Δ_{V_μ} and Δ_{A_μ} defined in (22) and (23).

We show the results for $\Delta_{V_\mu}(E_1^{(0)}, E_2^{(0)}, r)$ in Fig. 7(a) for $E_1^{(0)} = E_2^{(0)}$ and in

Fig. 7(b) for $E_1^{(0)} = 0$ for the $r = 1$ case. For both cases the values for Δ_{V_i} are close to those for Δ_{V_4} below $E_2^{(0)} \lesssim 0.01$, beyond which Δ_{V_4} decreases in magnitude, whereas Δ_{V_i} increases. In the heavy quark mass region $E_2^{(0)} \approx O(1 - 2)$, where current b -quark simulations are performed, the values of Δ_{V_i} and Δ_{V_4} deviate by about 100% from those at $E_2^{(0)} = 0$.

For the axial vector current the results for $\Delta_{A_\mu}(E_1^{(0)}, E_2^{(0)}, r)$ are plotted in Fig. 8(a) for $E_1^{(0)} = E_2^{(0)}$ and in Fig. 8(b) for $E_1^{(0)} = 0$, again for the $r = 1$ case. We observe that the characteristic features for the $E_2^{(0)}$ dependence of Δ_{A_μ} are similar to those of Δ_{V_μ} , where Δ_{A_i} corresponds to Δ_{V_4} and Δ_{A_4} to Δ_{V_i} . We note that Δ_{A_i} and Δ_{A_4} also suffer from a 100% $m_q a$ correction in the heavy quark region $E_2^{(0)} \approx O(1 - 2)$.

6 Conclusions and discussion

In this paper we have calculated the one-loop contributions for the renormalization factors of the vector and axial vector currents including finite quark mass corrections using the Wilson quark action. We have demonstrated that the one-loop contributions suffer from a very large correction of $O(100\%)$ for the heavy quark masses of order unity in lattice units, which corresponds to the situation of current b -quark simulations. This fact tells us that the $m_q a$ corrections should be incorporated even at the one-loop level for the renormalization factors of the weak operators containing the b -quarks in current numerical simulations using the Wilson quark action.

In this work our investigation has been concentrated on the Wilson quark action, which is the most naive, unimproved, quark action on the lattice. We wonder how large the $m_q a$ corrections are for improved quark actions at the one-loop level. This point should be examined through a calculation similar to ours including finite quark mass contributions, which we leave for future investigations.

Acknowledgement

We thank S. Aoki for useful discussions, and A. Ukawa for valuable comments and careful reading of the manuscript. This work is supported in part by Grants-in-Aid of the Ministry of Education (No.08740221).

Appendix

In this appendix we present expressions of the continuum one-loop vertex corrections and the integrals of the counter terms introduced to regularize the IR divergence of the one-loop lattice vertex corrections for some specified cases of the pole masses.

We first list expressions of the continuum vertex corrections $\Lambda_\Gamma^{(1)}(m_1, m_2)$ ($\Gamma = \gamma_\mu, \gamma_\mu \gamma_5$) for the case of $m_2 \rightarrow m_1$ and $m_1 \rightarrow 0$ with the assumption $\lambda < m_1, m_2$. From (89), (90), (94) and (95) we find that the vertex corrections are written in the following forms

$$\begin{aligned} & \lim_{m_2 \rightarrow m_1} \Lambda_\Gamma^{(1)}(m_1, m_2) / \left[\frac{C_F}{4\pi} \Gamma \right] \\ &= \left(\frac{2}{\epsilon} - \gamma + \ln |4\pi| \right) + \ln \left| \frac{\mu^2}{m_1^2} \right| + 2 \ln \left| \frac{\lambda^2}{m_1^2} \right| + C_0^{hh} + C_1 \frac{\pi m_1}{\lambda} \end{aligned} \quad (98)$$

and

$$\begin{aligned} & \lim_{m_1 \rightarrow 0} \Lambda_\Gamma^{(1)}(m_1, m_2) / \left[\frac{C_F}{4\pi} \Gamma \right] \\ &= \left(\frac{2}{\epsilon} - \gamma + \ln |4\pi| \right) + \ln \left| \frac{\mu^2}{m_1^2} \right| + 2 \ln \left| \frac{\lambda^2}{m_1^2} \right| + C_0^{hl} + C_1 \frac{\pi}{\lambda} \frac{2m_1 m_2}{m_1 + m_2}, \end{aligned} \quad (99)$$

where C_0 and C_1 are constants independent of m_1 and m_2 , which are tabulated in Table. 4.

We also enumerate expressions of the integrals of the counter terms to the lattice vertex corrections $\int_{-\pi}^{\pi} d^4 k / (2\pi)^4 \tilde{I}_\Gamma(k, \tilde{m}_1, \tilde{m}_2)$ ($\Gamma = \gamma_\mu, \gamma_\mu \gamma_5$) for the case of $\tilde{m}_2 \rightarrow \tilde{m}_1$ and $\tilde{m}_1 \rightarrow 0$ with the assumption $\lambda < \tilde{m}_1, \tilde{m}_2$. From (75), (76), (83)

and (84) we obtain the following expressions

$$\begin{aligned}
& \lim_{\tilde{m}_2 \rightarrow \tilde{m}_1} \int_{-\pi}^{\pi} \frac{d^4 k}{(2\pi)^4} \tilde{I}_{\Gamma}(k, \tilde{m}_1, \tilde{m}_2) / \left[\frac{C_F}{4\pi} \Gamma \right] \\
= & 2 \ln \left| \frac{\lambda^2}{\Lambda^2} \right| + 6 \ln \left| \frac{\Lambda + \sqrt{\Lambda^2 + 4\tilde{m}_1^2}}{2\tilde{m}_1} \right| \\
& + C_1 \left[\frac{\pi \tilde{m}_1}{\lambda} - \frac{\sqrt{\Lambda^2 + 4\tilde{m}_1^2}}{\Lambda} \right] + C_2^{hh} \frac{\Lambda^2}{\tilde{m}_1^2} \\
& + C_3^{hh} \left[\frac{\Lambda^4}{\tilde{m}_1^4} - \frac{\Lambda}{\tilde{m}_1^4} (\Lambda^2 + 4\tilde{m}_1^2)^{\frac{3}{2}} \right] + (6C_3^{hh} - C_2^{hh}) \frac{\Lambda}{\tilde{m}_1^2} \sqrt{\Lambda^2 + 4\tilde{m}_1^2}, \quad (100)
\end{aligned}$$

whose massless limit is

$$\begin{aligned}
& \lim_{\tilde{m}_1 \rightarrow 0} \int_{-\pi}^{\pi} \frac{d^4 k}{(2\pi)^4} \tilde{I}_{\Gamma}(k, \tilde{m}_1, \tilde{m}_1) / \left[\frac{C_F}{4\pi} \Gamma \right] \\
= & \ln \left| \frac{\Lambda^2}{\tilde{m}_1^2} \right| + 2 \ln \left| \frac{\lambda^2}{\tilde{m}_1^2} \right| + C_0^l + C_1 \frac{\pi \tilde{m}_1}{\lambda}, \quad (101)
\end{aligned}$$

and

$$\begin{aligned}
& \lim_{\tilde{m}_1 \rightarrow 0} \int_{-\pi}^{\pi} \frac{d^4 k}{(2\pi)^4} \tilde{I}_{\Gamma}(k, \tilde{m}_1, \tilde{m}_2) / \left[\frac{C_F}{4\pi} \Gamma \right] \\
= & \ln \left| \frac{\Lambda^2}{\tilde{m}_1^2} \right| + 2 \ln \left| \frac{\lambda^2}{\tilde{m}_1^2} \right| \\
& - 3 + C_1 \frac{\pi}{\lambda} \frac{2\tilde{m}_1 \tilde{m}_2}{\tilde{m}_1 + \tilde{m}_2} + C_2^{hl} \frac{\Lambda^2}{\tilde{m}_2^2} + \frac{C_2^{hl}}{6} \left[\frac{\Lambda^4}{\tilde{m}_2^4} - \frac{\Lambda}{\tilde{m}_2^4} (\Lambda^2 + 4\tilde{m}_2^2)^{\frac{3}{2}} \right]. \quad (102)
\end{aligned}$$

where C_0, \dots, C_3 are constants independent of \tilde{m}_1 and \tilde{m}_2 , which are summarized in Table. 5.

References

- [1] K. Symanzik, Nucl. Phys. **B226** (1983) 187.
- [2] K. G. Wilson and J. Kogut, Phys. Reports **12C** (1974) 75.
- [3] For a review, see, *e.g.*, C. J. Morningstar, Nucl. Phys. **B** (Proc. Suppl.) **47** (1996) 92.
- [4] For a review, see, *e.g.*, G. C. Rossi, Nucl. Phys. **B** (Proc. Suppl.) **53** (1997) 3.
- [5] P. B. Mackenzie, Nucl. Phys. **B** (Proc. Suppl.) **30** (1993) 35; A. S. Kronfeld, *ibid.* **30** (1993) 445.
- [6] A. S. Kronfeld and B. P. Mertens, Nucl. Phys. **B** (Proc. Suppl.) **34** (1994) 495.
- [7] C. Bernard, T. Draper and A. Soni, Phys. Rev. D**36** (1987) 3224.
- [8] G. P. Lepage and P. B. Mackenzie, Phys. Rev. D**48** (1993) 2250.
- [9] S. Kawabata, Comput. Phys. Commun. **41** (1986) 127; *ibid.* **88** (1995) 309.

Tables

Table 1: $E^{(0)}$ dependence of $E^{(1)\text{latt}}(E^{(0)}, r)$ and $\Delta_\psi(E^{(0)}, r)$. The Wilson parameter r is chosen to be one. The error in the numerical integration is less than 2%.

$E^{(0)}$	$E^{(1)\text{latt}}$	Δ_ψ
0	0	-6.90×10^{-2}
0.001	4.96×10^{-3}	-6.83×10^{-2}
0.01	3.39×10^{-2}	-8.30×10^{-2}
0.1	1.80×10^{-1}	-1.59×10^{-1}
0.2	2.66×10^{-1}	-2.07×10^{-1}
0.5	3.99×10^{-1}	-2.83×10^{-1}
1	5.13×10^{-1}	-2.98×10^{-1}
2	6.68×10^{-1}	-2.43×10^{-1}

Table 2: (a) $\Delta_{\gamma_i}(E_1^{(0)}, E_2^{(0)}, r)$ and (b) $\Delta_{\gamma_4}(E_1^{(0)}, E_2^{(0)}, r)$ for combinations of $E_1^{(0)}$ and $E_2^{(0)}$. The Wilson parameter r is chosen to be one. The error in the numerical integration is less than 2%.

(a) $\Delta_{\gamma_i}(i = 1, 2, 3)$								
$E_2^{(0)}$	$E_1^{(0)}$							
	0	0.001	0.01	0.1	0.2	0.5	1	2
0	-8.29×10^{-1}							
0.001	-8.30×10^{-1}	-8.31×10^{-1}						
0.01	-8.43×10^{-1}	-8.44×10^{-1}	-8.58×10^{-1}					
0.1	-9.18×10^{-1}	-9.11×10^{-1}	-9.28×10^{-1}	-9.94×10^{-1}				
0.2	-9.71×10^{-1}	-9.66×10^{-1}	-9.82×10^{-1}	-1.04	-1.08			
0.5	-1.08	-1.07	-1.09	-1.14	-1.16	-1.19		
1	-1.18	-1.18	-1.20	-1.27	-1.31	-1.31	-1.31	
2	-1.32	-1.32	-1.35	-1.46	-1.54	-1.69	-1.77	-2.12
(b) Δ_{γ_4}								
$E_2^{(0)}$	$E_1^{(0)}$							
	0	0.001	0.01	0.1	0.2	0.5	1	2
0	-8.19×10^{-1}							
0.001	-8.24×10^{-1}	-8.19×10^{-1}						
0.01	-8.13×10^{-1}	-8.11×10^{-1}	-8.06×10^{-1}					
0.1	-7.31×10^{-1}	-7.33×10^{-1}	-7.30×10^{-1}	-6.92×10^{-1}				
0.2	-6.50×10^{-1}	-6.55×10^{-1}	-6.53×10^{-1}	-6.38×10^{-1}	-6.03×10^{-1}			
0.5	-4.57×10^{-1}	-4.51×10^{-1}	-4.62×10^{-1}	-4.81×10^{-1}	-4.74×10^{-1}	-4.00×10^{-1}		
1	-2.19×10^{-1}	-2.16×10^{-1}	-2.18×10^{-1}	-2.55×10^{-1}	-2.69×10^{-1}	-2.48×10^{-1}	-1.75×10^{-1}	
2	$+7.40 \times 10^{-2}$	$+7.20 \times 10^{-2}$	$+6.96 \times 10^{-2}$	$+3.58 \times 10^{-2}$	$+9.03 \times 10^{-3}$	-2.73×10^{-2}	-2.31×10^{-2}	$+3.20 \times 10^{-2}$

Table 3: (a) $\Delta_{\gamma_i\gamma_5}(E_1^{(0)}, E_2^{(0)}, r)$ and (b) $\Delta_{\gamma_4\gamma_5}(E_1^{(0)}, E_2^{(0)}, r)$ for combinations of $E_1^{(0)}$ and $E_2^{(0)}$. The Wilson parameter r is chosen to be one. The error in the numerical integration is less than 2%.

(a) $\Delta_{\gamma_i\gamma_5}(i = 1, 2, 3)$								
$E_2^{(0)}$	$E_1^{(0)}$							
	0	0.001	0.01	0.1	0.2	0.5	1	2
0	-3.13×10^{-1}							
0.001	-3.14×10^{-1}	-3.12×10^{-1}						
0.01	-3.08×10^{-1}	-3.05×10^{-1}	-2.99×10^{-1}					
0.1	-2.71×10^{-1}	-2.62×10^{-1}	-2.66×10^{-1}	-2.44×10^{-1}				
0.2	-2.43×10^{-1}	-2.33×10^{-1}	-2.40×10^{-1}	-2.27×10^{-1}	-2.17×10^{-1}			
0.5	-1.91×10^{-1}	-1.85×10^{-1}	-1.83×10^{-1}	-1.88×10^{-1}	-1.90×10^{-1}	-1.88×10^{-1}		
1	-1.31×10^{-1}	-1.25×10^{-1}	-1.24×10^{-1}	-1.31×10^{-1}	-1.43×10^{-1}	-1.58×10^{-1}	-1.49×10^{-1}	
2	-2.87×10^{-2}	-3.00×10^{-2}	-3.04×10^{-2}	-4.94×10^{-2}	-6.66×10^{-2}	-1.04×10^{-1}	-1.24×10^{-1}	-1.21×10^{-1}
(b) $\Delta_{\gamma_4\gamma_5}$								
$E_2^{(0)}$	$E_1^{(0)}$							
	0	0.001	0.01	0.1	0.2	0.5	1	2
0	-3.15×10^{-1}							
0.001	-3.15×10^{-1}	-3.14×10^{-1}						
0.01	-3.09×10^{-1}	-3.06×10^{-1}	-3.03×10^{-1}					
0.1	-2.90×10^{-1}	-2.83×10^{-1}	-2.82×10^{-1}	-2.61×10^{-1}				
0.2	-2.88×10^{-1}	-2.78×10^{-1}	-2.82×10^{-1}	-2.60×10^{-1}	-2.53×10^{-1}			
0.5	-3.36×10^{-1}	-3.26×10^{-1}	-3.36×10^{-1}	-3.25×10^{-1}	-3.10×10^{-1}	-3.13×10^{-1}		
1	-4.83×10^{-1}	-4.74×10^{-1}	-4.89×10^{-1}	-5.15×10^{-1}	-5.21×10^{-1}	-4.99×10^{-1}	-5.46×10^{-1}	
2	-8.16×10^{-1}	-8.20×10^{-1}	-8.38×10^{-1}	-9.27×10^{-1}	-1.00	-1.12	-1.20	-1.61

Table 4: Coefficients C_0 and C_1 in the continuum vertex corrections for the cases of $m_2 \rightarrow m_1$ and $m_1 \rightarrow 0$.

Γ	C_0^{hh}	C_1	C_0^{hl}
γ_i	-4	+4	-4
γ_4	+4	0	-2
$\gamma_i\gamma_5$	+2	0	-4
$\gamma_4\gamma_5$	-2	+4	-2

Table 5: Coefficients C_0, \dots, C_3 in the lattice vertex corrections for the cases of $\tilde{m}_2 \rightarrow \tilde{m}_1$ and $\tilde{m}_1 \rightarrow 0$.

Γ	C_1	C_2^{hh}	C_3^{hh}	C_0^{ll}	C_2^{hl}
γ_i	+4	0	+1/12	-7/2	+1/2
γ_4	0	0	+3/4	+9/2	-3/2
$\gamma_i\gamma_5$	0	-2	-1/4	+5/2	+1/2
$\gamma_4\gamma_5$	+4	-2	-1/4	-3/2	-3/2

Figure Captions

Fig. 1 One-loop diagram for the quark self-energy. k is the loop momentum and p is the external quark momentum.

Fig. 2 One-loop correction to the pole mass on the lattice as a function of $E^{(0)}$. The Wilson parameter r is chosen to be one. Open symbol denotes the value at $E^{(0)} = 0$.

Fig. 3 One-loop coefficient of the relation between the on-shell wave-function renormalization factors on the lattice and in the continuum with NDR scheme as a function of $E^{(0)}$. The Wilson parameter r is chosen to be one. Open symbol denotes the value at $E^{(0)} = 0$.

Fig. 4 One-loop diagrams for the vertex corrections. k is the loop momentum and p is the incoming quark momentum. p' denotes the outgoing quark momentum for (a) and the incoming anti-quark momentum for (b).

Fig. 5 One-loop coefficients of the relation between the vertex corrections for γ_μ on the lattice and in the continuum with NDR scheme. (a) is for the case of $E_1^{(0)} = E_2^{(0)}$ and (b) for $E_1^{(0)} = 0$. The Wilson parameter r is chosen to be one. Open symbols denote the values at $E^{(0)} = 0$.

Fig. 6 One-loop coefficients of the relation between the vertex corrections for $\gamma_\mu\gamma_5$ on the lattice and in the continuum with NDR scheme. (a) is for the case of $E_1^{(0)} = E_2^{(0)}$ and (b) for $E_1^{(0)} = 0$. The Wilson parameter r is chosen to be one. Open symbols denote the values at $E^{(0)} = 0$.

Fig. 7 One-loop coefficients of the renormalization factors for vector currents. (a) is for the case of $E_1^{(0)} = E_2^{(0)}$ and (b) for $E_1^{(0)} = 0$. The Wilson parameter r is chosen to be one. Open symbols denote the values at $E^{(0)} = 0$.

Fig. 8 One-loop coefficients of the renormalization factors for axial vector currents.

(a) is for the case of $E_1^{(0)} = E_2^{(0)}$ and (b) for $E_1^{(0)} = 0$. The Wilson parameter r is chosen to be one. Open symbols denote the values at $E^{(0)} = 0$.

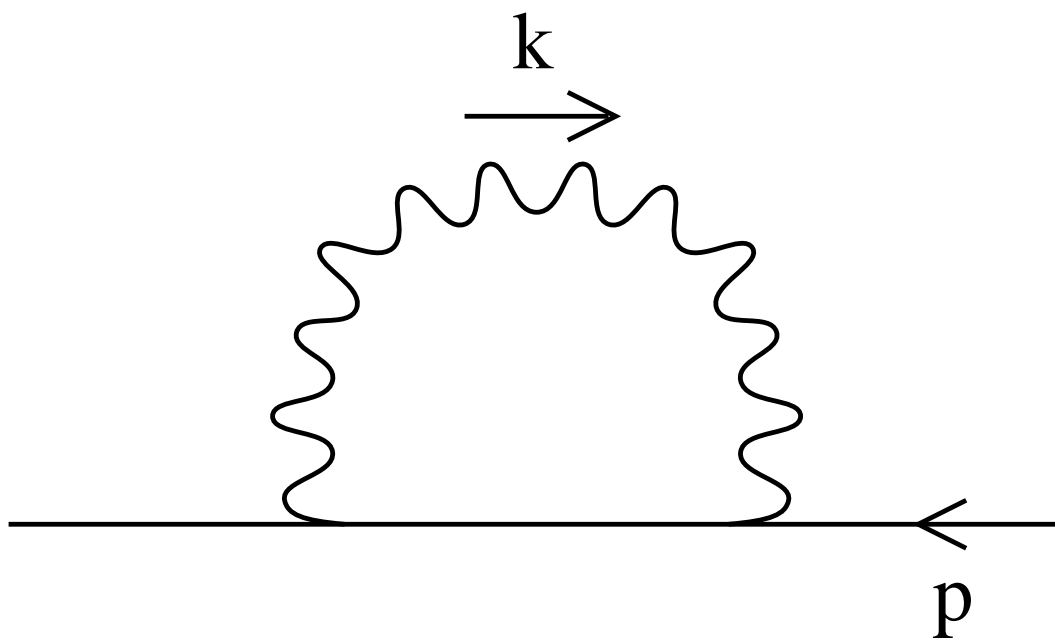


Fig. 1

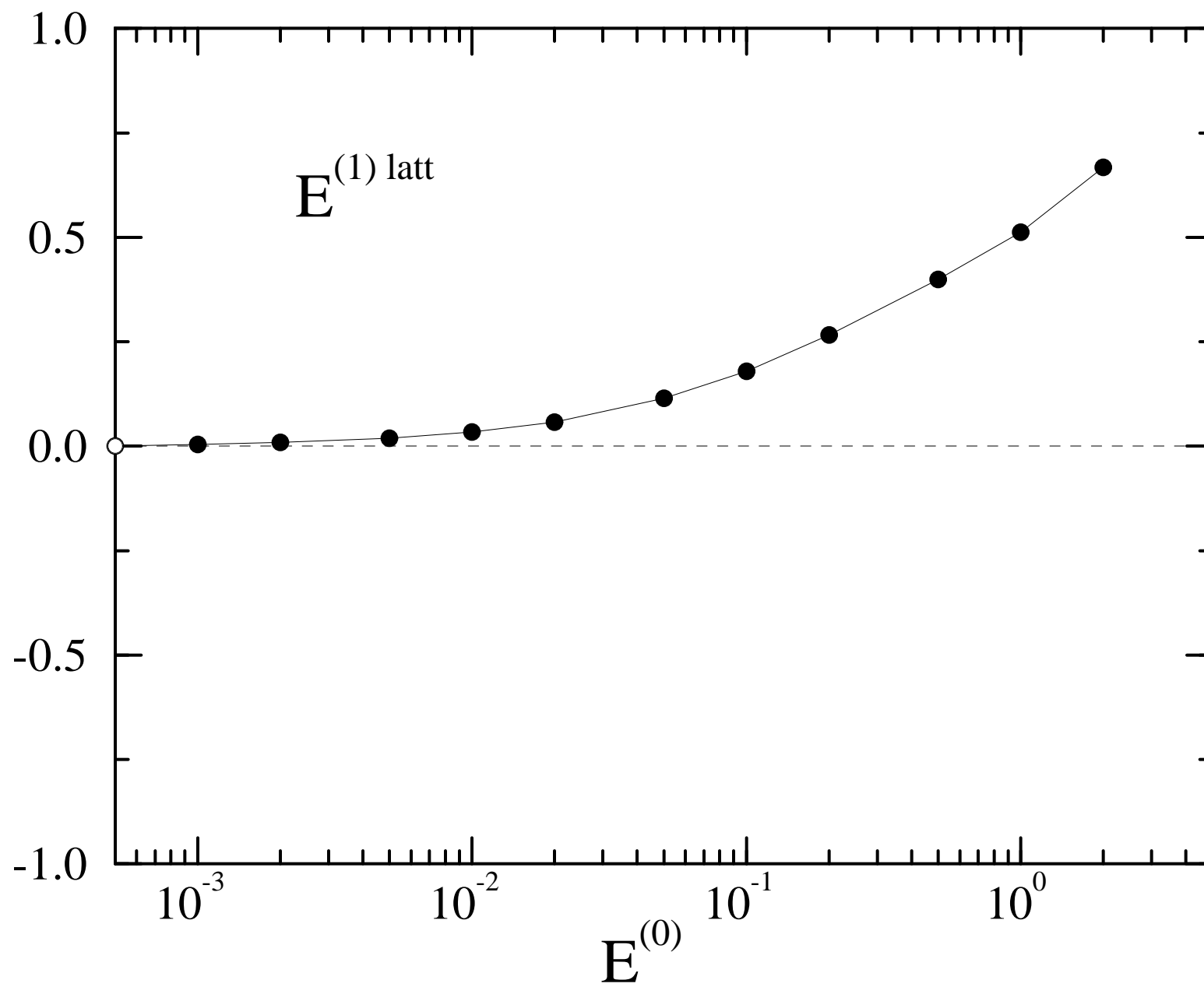


Fig. 2

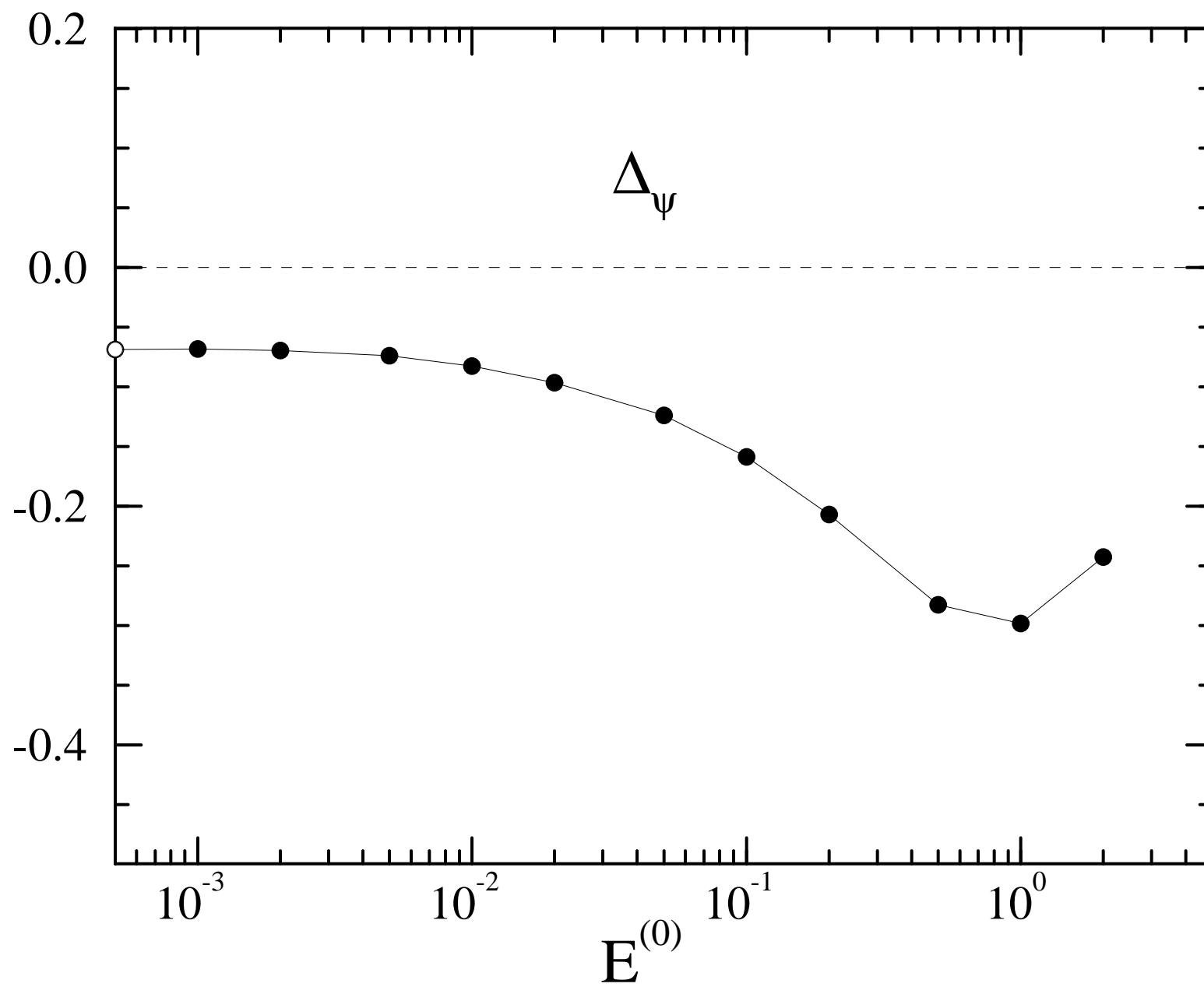
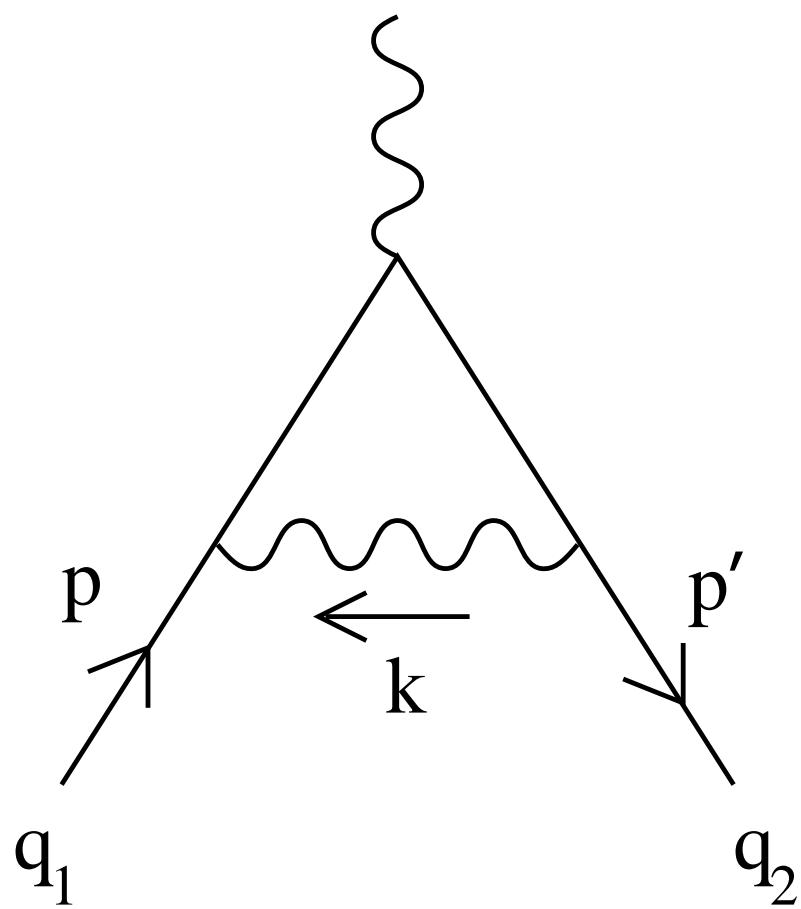
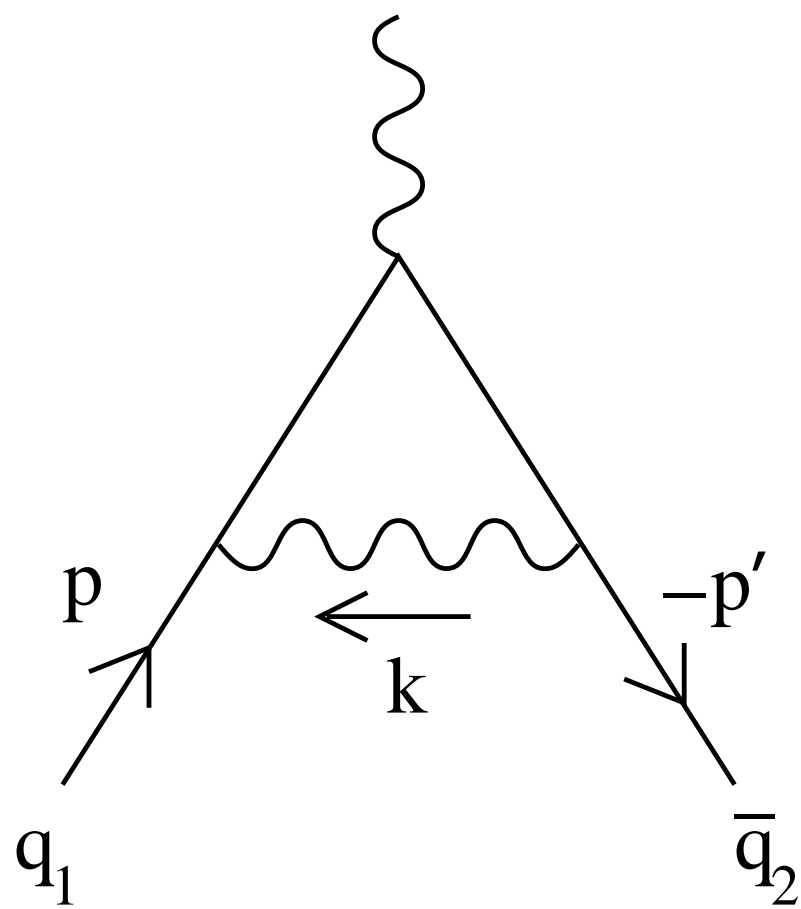


Fig. 3



(a)



(b)

Fig. 4

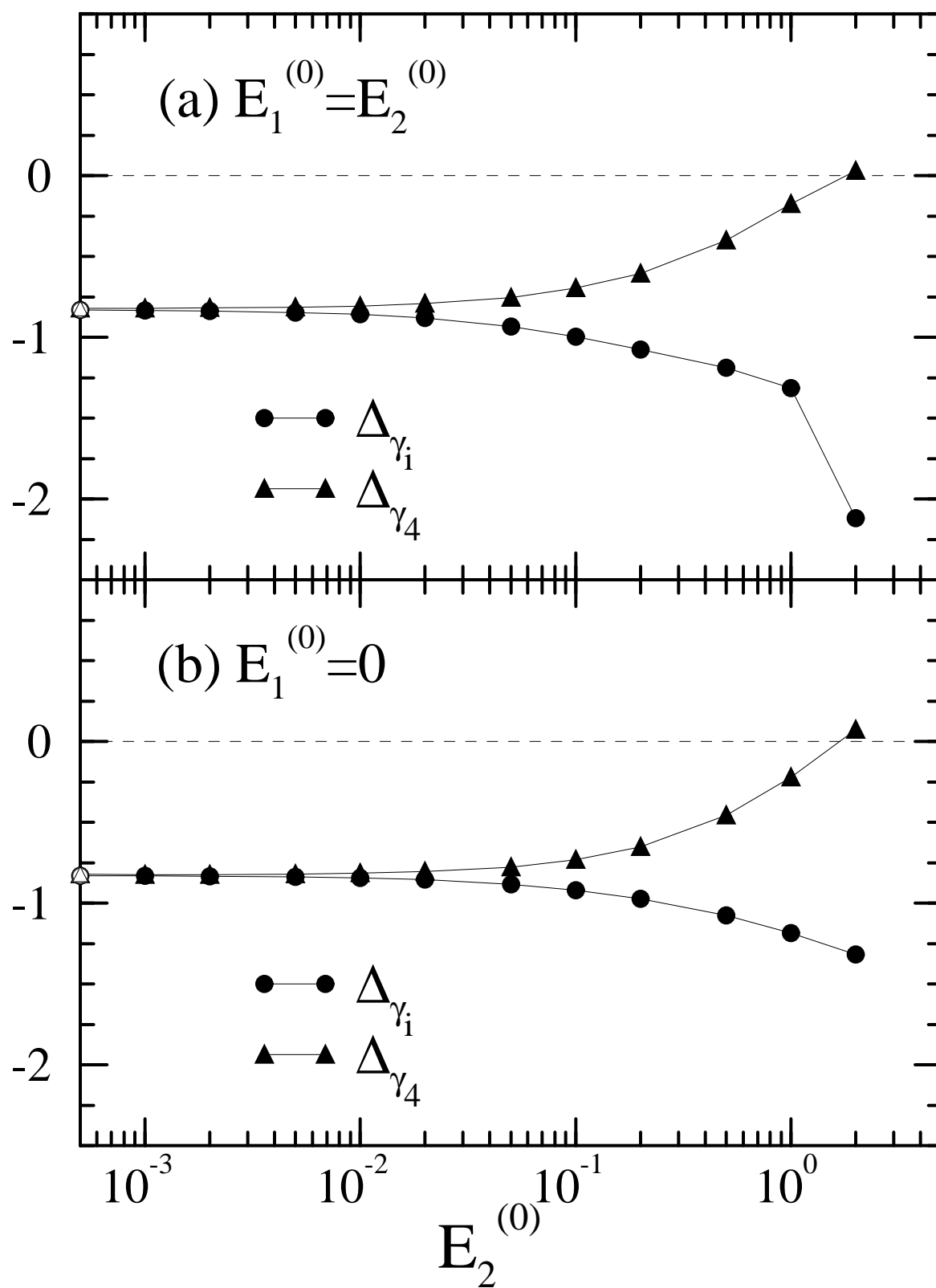


Fig. 5

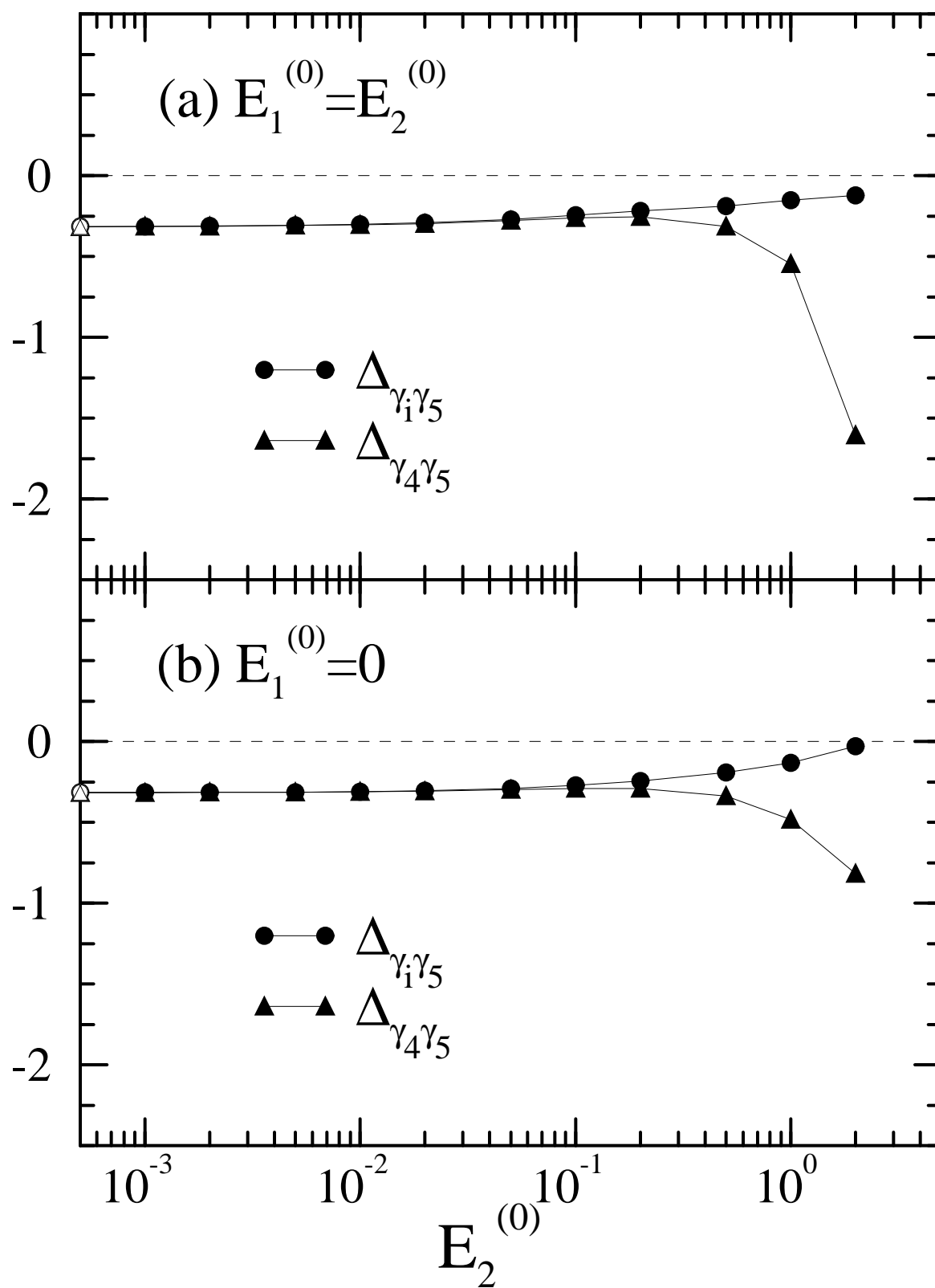


Fig. 6

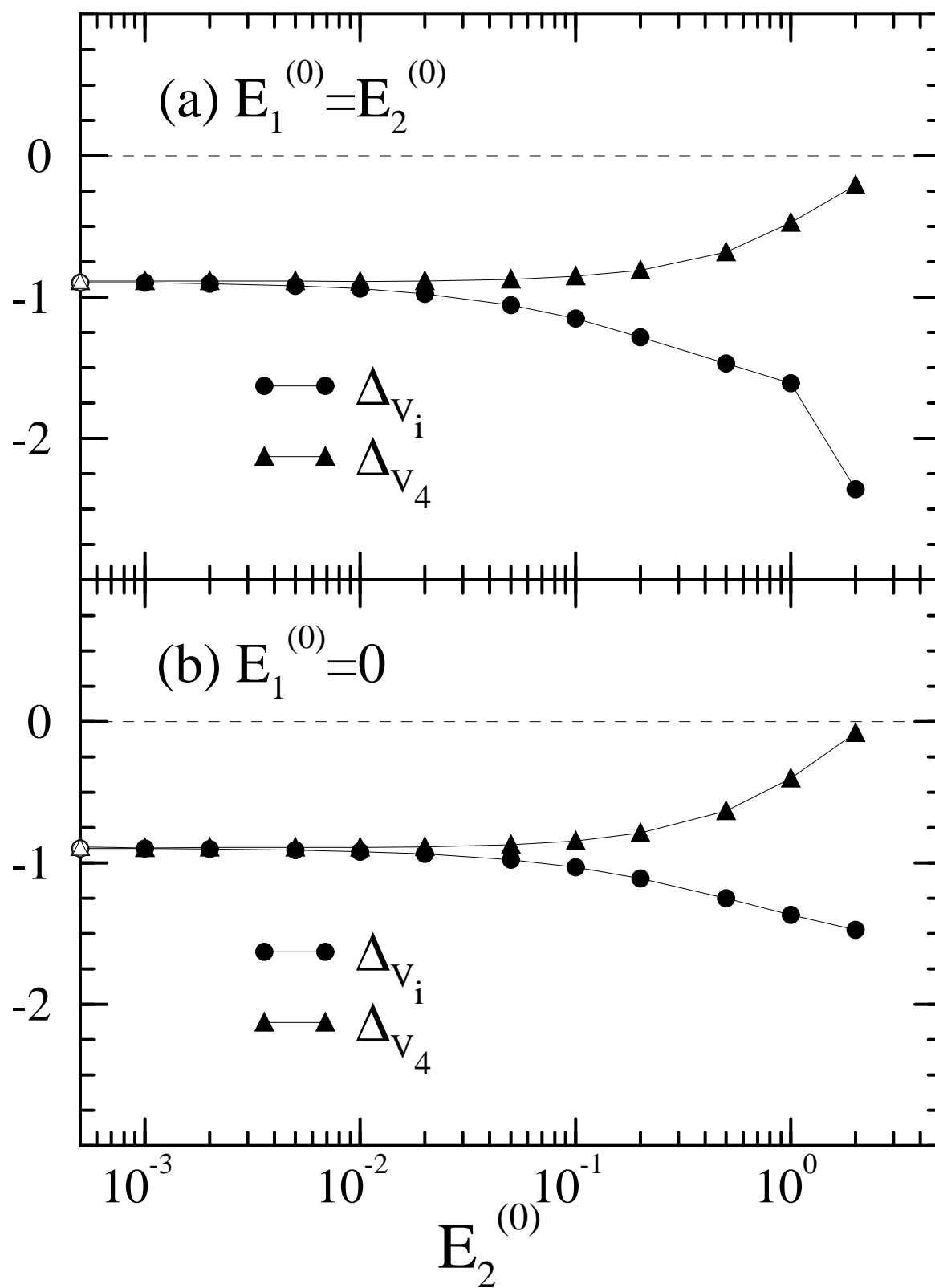


Fig. 7

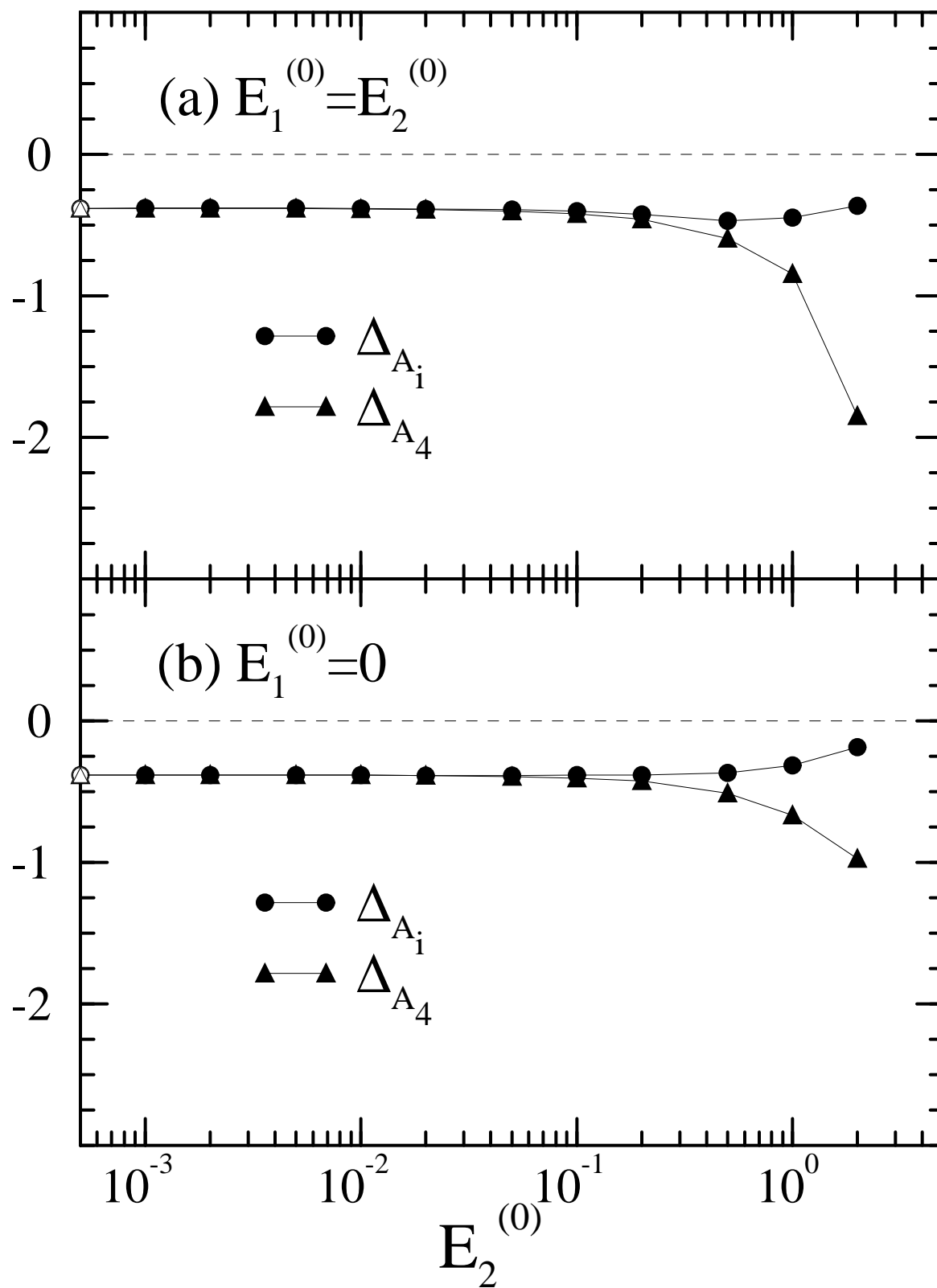


Fig. 8